Impact of Bluetooth Interference on the Performance of IEEE 802.11b Wireless LAN

by

Anirudha A Vaidya

Problem Report submitted to the
College of Engineering and Mineral Resources
at West Virginia University
in partial fulfillment of the requirements
for the degree of

Master of Science
in
Electrical Engineering

Daryl S. Reynolds, Ph.D., Chair
Matthew C. Valenti, Ph.D.
Wils L. Cooley, Ph.D.

Lane Department of Computer Science and Electrical Engineering

Morgantown, West Virginia
2004

Keywords: 802.11b, WLAN, Bluetooth, Throughput, Interference Cancellation, Channel Estimation, Throughput Optimization, Space Time Codes, Large and Small Scale Fading

Abstract

Impact of Bluetooth Interference on the Performance of IEEE 802.11b Wireless LAN

by

Anirudha A Vaidya
Master of Science in Electrical Engineering

West Virginia University

Daryl S. Reynolds, Ph.D., Chair

Wireless radio technologies such as IEEE 802.11 and Bluetooth operating in the 2.4 GHz unlicensed frequency band lead to signal interference and performance degradation when operating at the same time. This project simulates the impact of Bluetooth interferers on the IEEE 802.11b wireless LAN. In particular the effect of Bluetooth interference on the network throughput of 802.11b using multiple transmit and receive antennas is observed.

We present an 802.11b throughput simulator with optimum packet sizes for a slow flat fading channel with upper and lower bounds on the best and worst case throughput in the presence of a Bluetooth interferer. The effect of using Maximal Ratio Combining with 1 Transmit - 2 Receive antennas and Space time Coding with 2 Transmit - 1 Receive antennas on the throughput of 802.11b is simulated. We observe the throughput improvement for lower values of signal to noise ratios by assuming error correcting capability. Finally, we attempt to cancel the interference due to Bluetooth and receiver noise by using an interference cancellation technique.

From our results, we can conclude that the throughput performance of the system improved with the use of multiple transmit/receive antennas over the single antenna transmit-receive system. The performance also improves with increasing distance between the Bluetooth interferer and the 802.11b receiver. The interference cancellation technique cancels out the harmful Bluetooth interference and increases the range of the system. Finally, we conclude with the scope for future work in this area.

Acknowledgments

I would like to thank my advisor, Dr Daryl S. Reynolds for his valuable and timely suggestions during this project. I would also like to thank my committee members, Dr. Matthew Valenti and Dr. Wils Cooley for their support.

My project would not be complete without the strong backing from my parents Mr Anil V. Vaidya and Mrs Ashwini A. Vaidya, my brother Kaustubh A. Vaidya and my relatives. A special thanks to all my friends here at West Virginia University and in India for their valuable comments.

Contents

List of Figures

List of Tables

Notation

We use the following notation and symbols throughout this problem report

ACK	:	Acknowledgement
AWGN	:	Additive White Gaussian Noise
BER	:	Bit Error Rate
CCK	:	Complementary Code Keying
CRC	:	Cyclic Redundancy Check
CSMA/CA	:	Carrier Sense Multiple Access with Collision Avoidance
CTS	:	Clear To Send
DPSK	:	Differential Phase Shift Keying
DSSS	:	Direct Sequence Spread Spectrum
DQPSK	:	Differential Quaternary Phase Shift Keying
FHSS	:	Frequency Hopping Spread Spectrum
HR/DSSS	:	High Rate Direct Sequence Spread Spectrum
IC	:	Interference Cancellation
IR	:	Infrared
ISM Band	:	Industrial Scientific Medicine Band
MAC	:	Medium Access Control
MRC	:	Maximal Ratio Combining
OFDM	:	Orthogonal Frequency Division Multiplexing
PBCC	:	Packet Binary Convolutional Coding
PER	:	Packet Error Rate
PHY	:	Physical Layer
PLCP	:	Physical Layer Convergence Protocol
PPDU	:	PHY Protocol Data Units
PSDU	:	PLCP Service Data Units
RTS	:	Ready To Send
RX	:	Receive Antenna
SNR	:	Signal to Noise Ratio
STC	:	Space Time Codes
TX	:	Transmit Antenna
$(.)^H$	:	denotes complex conjugate transpose
$(.)^*$	:	denotes complex conjugate

Chapter 1

Interference in the 2.4 GHz ISM Band

Over the years, the ease of wireless connectivity has made the wireless technologies increasingly popular and cost effective. The future foresees an ever increasing number of voice and data applications in personal, home and office environments functioning without the use of cables. The functional specifications and bandwidth requirements of the different Wireless Area Networking (WAN) technologies make it difficult for any single wireless technology to serve all the available applications in the most optimal way. Depending on the applications, the use of different technologies with specific strengths to achieve optimal results is justified.

Bluetooth (BT)[8] and IEEE 802.11x [9] are the two wireless standards that have become increasingly popular in the industry. Bluetooth and IEEE 802.11b complement each other due to their co-existence in the 2.4 GHz unlicensed Industrial Scientific Medicine (ISM) band. The rapid advancements and growth of Bluetooth technology has made the issue of co-existence between different wireless devices an increasingly significant and important topic of discussion and analysis.

1.1 Interference Sources in the 2.4 GHz band

Microwave ovens in residential areas are one of the first sources of interference in the 2.4 GHz band. With the advent of newer cordless phones, the interference scenario in the 2.4 GHz band has become an interesting topic of research and analysis. The popularity of newer communication devices equipped with Bluetooth radios, has raised questions regarding their

impact on the throughput of wireless LANs. The 2.4 GHz ISM band is thus becoming "busier" day by day.

1.2 Bluetooth Background

Bluetooth is a small-range (0-10 m) low-power radio link between two devices operating in the unlicensed 2.4-GHz industrial scientific and medical (ISM) band. The future of Bluetooth revolves around the issue of extending its range beyond 30 feet. This can be done by increasing its transmit power from 1mW to 100 mW.

Bluetooth radios transmit short packets using Frequency Hopping Spread Spectrum (FHSS) at a hop-rate of 1600 hops/second. The use of fast hopping means that Bluetooth spends little time on any channel which might be experiencing interference. This has the advantage of better network performance while giving rise to reduced throughput due to time wasted during the hops. The Bluetooth device has been described as a "bad neighbor" in the 2.4 GHz band mainly due to the absence of a listen-before-talk protocol. The Bluetooth node transmits blindly whenever its timing dictates, not worrying about the possibility that the channel frequency might be in use by another system. Thus, the analysis of Bluetooth interference assumes significance while evaluating the performance of an 802.11b wireless LAN.

1.3 IEEE 802.11b Background

The popular IEEE 802.11b 'wireless LAN' is functional mostly in offices, campus and residential environments. The IEEE 802.11 standard defines 3 different Physical Layer (PHY) specifications namely; Frequency Hopping Spread Spectrum (FHSS), Direct Sequence Spread Spectrum (DSSS) and Infrared (IR). The IEEE 802.11b is based on the DSSS PHY technique. DSSS systems transmit on a fixed co-allocated channel by spreading the signal with a pseudorandom (PN) sequence. The signal spreading aims to combat narrow band interference. However, the DSSS system can be helpless in severe interference situations due to its static (non-hopping) nature. In contrast, an FHSS system can hop around the interfering

signal while experiencing only small degradation in the throughput.

The 802.11b standard defines an 11-bit Barker sequence with a chipping rate of 11 Mchips/sec for DSSS spreading with 1 and 2 Mbps data rates. The 1 Mbps DPSK uses DSSS spreading with a symbol rate of 1 MSps. The 11 Mbps CCK uses 8-chip coding with a symbol rate of 1.375 MSps and a chipping rate of 11 Mchips/s. This technique makes the CCK signal occupy the same bandwidth as the lower rates.

The bandwidth of the spread signal is 22 MHz on a single channel Thus, in the 83.5 MHz bandwidth of the ISM band, with a frequency spacing of 17.5 MHz, a maximum of 3 channels can be accommodated. Certain countries like France and Spain allow only for only one non-overlapping channel.

1.4 Previous Work

Researchers have toiled to develop some tools for wireless network simulation [10]. These tools are basically a PHY implementation of the standards abstracted to a discrete time channel model. Based on this work, N. Golmie and R.E.Van Dyck [11] designed models in C and OPNET and suggested the use of an integrated PHY-MAC model to capture the effects of interference simultaneously in the time and frequency domains. Kamerman [12] obtained experimental results on the interference between 802.11b and Bluetooth. The analytical approach to address the problem of calculating the probability of 802.11b packet error in the presence of Bluetooth interference was first proposed by Ennis [13], then extended by Zyren [14] and Shellhammer [15]. Chiasserini and Rao [16] suggested the use of traffic shaping techniques to reduce the impact of BT data and voice on the 802.11b performance. In contrast, Golmie and Mouveaux [17] used a probabilistic approach to study the impact of 802.11 on Bluetooth. Henricksson [18] suggested the use of spatial diversity on WLAN receivers to reduce the Bluetooth interference on the IEEE 802.11b LAN. Michael Fainberg and David Goodman [1] analyzed and derived the throughput performance of 802.11b with BT interference in an office and home environment and presented techniques for throughput optimization. Conversely, I. Howitt presented analytical expressions for Bluetooth performance in the presence of WLAN [19].

We aim to collect data from all the sources mentioned above and present simple models for evaluating the 802.11b network performance with Bluetooth. Our work focusses on the analysis and simulation of the 802.11b and Bluetooth PHY layers with the necessary system parameters and evaluating the network performance of the IEEE 802.11b.

1.5 Contribution of this Project

This problem report analyzes the impact of Bluetooth interference on the performance of IEEE 802.11b Wireless LAN. We study the impact of Bluetooth on the Bit-Error-Rate (BER) performance of the 802.11b with different receiver designs namely the single antenna and the Maximal Ratio Combining (MRC) receivers. The effect of using 2 transmit antennas (space time codes) in achieving better performance is also observed. The Bluetooth interference limits the performance of the 802.11b system by giving rise to an error floor. We aim to reduce the Bluetooth interference with the use of an Interference Rejection Cancellation (IRC) scheme with channel estimation. The impact of Bluetooth interference on the throughput of 802.11b is analyzed. Choosing the best optimum packet size for each modulation scheme gives us the best possible throughput in the presence and absence of any external interference. With all the simulation parameters thus derived, we present an 802.11b simulator with upper and lower bounds on the best and the worst possible throughput with Bluetooth interference.

1.6 Organization of the Report

In Chapter 2 we briefly describe the IEEE 802.11b Wireless LAN PHY and MAC layers. Chapter 3 gives an account of the modulation schemes, with performances in Additive White Gaussian Noise (AWGN) and slow flat fading channels. An overview of the Bluetooth system and GFSK modulation used in Bluetooth is presented in chapter 4. Chapter 5 explains the interference model used in the simulations. In Chapter 6, we characterize the channel model used for the throughput analysis. In chapter 7, we present the results of throughput analysis in a flat fading channel and try to optimize the throughput for each of the data rates. In chapter 8, we decide on the network topology used in the throughput analysis

and optimization in the presence of Bluetooth interference. The throughput analysis and optimization in the presence of BT interferers is presented in chapter 9, similar to chapter 7. Finally using optimized packet sizes, we present the 802.11b throughput simulator in chapter 10 and test its performance for various receiver designs.

Chapter 2

The IEEE 802.11b Wireless LAN

2.1 Introduction

This section introduces the wireless local area networks (WLANs) with respect to the mobility challenges in these systems and its various topologies. Mobility is the most desirable characteristic of wireless networks, which in turn is influenced by numerous challenges in the wireless medium taking place at the layers of OSI model. The decision regarding the transmission technology (RF or IR) has to be made at the physical layer. The data link layer has to account for fading radio channels with burst errors. The problems encountered at these two layers increase the difficulty of achieving reliable communications.

The design of these two layers, thus, fell on the 802.11 [20, 21, 9] and 802.15 [22] subgroups leading to the evolution of IEEE 802.11 standard. Wireless LANs have been standardized by the IEEE 802.11 standards subgroup formed originally in 1987. The final approval for the 802.11 was obtained in 1997 for local wireless connectivity. The IEEE 802.11 lists out the "media access control (MAC) and physical layer specifications for wireless connectivity for fixed, portable and movable stations within a local area" [23]. The technologies used for wireless LANs exist in the ISM bands: 2.4-2.4835 GHz, 5.15-5.35 GHz, and 5.725-5.825 GHz. Multiple user separation in wireless LANs is carried out using Carrier Sense Multiple Access (CSMA) protocol. The spreading techniques used can be divided into two categories: FHSS and DSSS, for interference suppression.

2.2 IEEE 802.11

In 1987, the IEEE standards committee formed the 802.11 Wireless Local Area Networks Standards Working Group. The primary task of this group was to develop a global standard for radio equipment and networks in the 2.4 GHz unlicensed ISM band, with data rates of 1 and 2 Mbps. With final approval from IEEE in 1997, the 802.11 standard was drafted. The 802.11 was developed originally for a 2 Mbps data rate using direct-sequence spread spectrum or frequency hoping spread spectrum. In 1999, a higher data rate standard - the 802.11b, with data rate of 11 Mbps, was developed using high rate direct sequence spread spectrum (HR/DSSS).

2.3 Network Topology

The IEEE 802.11 standard supports three basic topologies: Independent Basic Services Set (IBSS), the Basic Service Set (BSS) and the Extended Service Set (ESS).

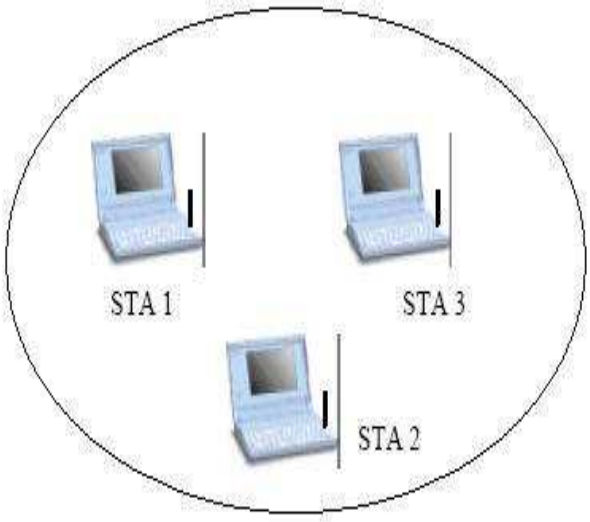

Figure 2.1: Independent Basic Service Set (IBSS) configuration reproduced from [1]

The BSS as shown in the Figure 2.1 consists of one or multiple wireless stations (STAs) communicating with each other. This situation is designated specially as an IBSS configuration. IBSS configurations are popularly referred to as Ad-Hoc networks, with direct

communication between the connected computers without any connection to a wired network.

A more flexible configuration of an BSS is the Infrastructure Mode, which consists of an Access Point (AP). The AP serves as a bridge between the wired and the wireless worlds. With the presence of an AP, the STAs do not communicate on a peer-to-peer basis, but instead use the access point(AP) to communicate between 2 STAs or between an STA and the wired network.

An ESS configuration as shown in the Figure 2.2 consists of numerous overlapping BSS connected by a distributed system, usually an Ethernet LAN. The STAs can roam from one BSS to another and communicate within the ESS.

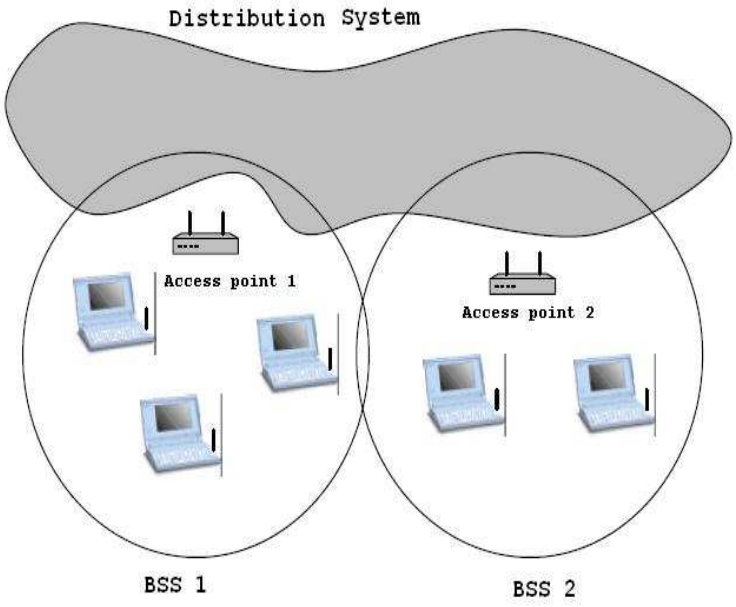

Figure 2.2: Extended Service Set(ESS) configuration reproduced from [1]

2.4 IEEE 802.11 PHY

The PHY layer is responsible for the transmission of data between the various nodes in a network. The IEEE 802.11 standard defines 5 different PHY specifications.

- Direct Sequence Spread Spectrum (DSSS)

- Frequency Hopping Spread Spectrum (FHSS)
- Infrared (IR)
- High Rate Direct Sequence Spread Spectrum (HR/DSSS)
- Orthogonal Frequency Division Multiplexing (OFDM)

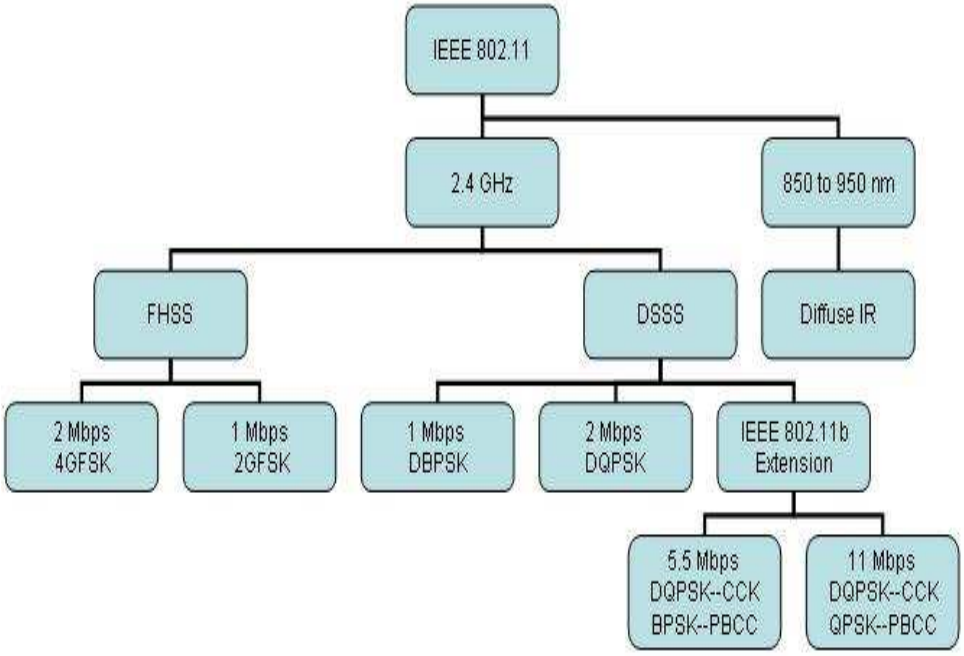

Figure 2.3: IEEE 802.11 PHY reproduced from [2]

In DSSS the signal waveform is spread around a wider bandwidth by multiplying the signal with a pseudorandom (PN) waveform. The spreading sequence used in 802.11 is an 11-chip Barker sequence. The channel bandwidth is thus raised to 22 MHz, making room for 3 non-overlapping channels in the 83.5 MHz ISM bandwidth. The data rates used for this technique are the 1 Mbps Differential Phase Shift Keying (DPSK) and the 2 Mbps Differential Quaternary Phase Shift Keying (DQPSK) [24, 3].

FHSS specifies a pseudo random frequency hopping sequence to transmit data packets in different frequency channels. By spreading the transmissions over frequency with time, the data is spread over a larger bandwidth. For FHSS, we have 79 channels of 1MHz in the

ISM band having a hop rate of 2.5 hops/sec. The data rates for this technique are 1 and 2 Mbps.

IR uses infrared light with a wavelength of about 850 to 950 nm to send data. This modulation scheme is in use only in indoor systems and requires line of sight propagation.

HR/DSSS uses Complementary Code Keying (CCK) [25, 26] to send data while occupying the same spectrum as the lower data rates. As the name suggests, HR/DSSS uses higher data rates of 5.5 Mbps and 11 Mbps. Using higher data rates requires higher signal to noise ratios (SNRs) which leads to a reduction in the range of operation for this scheme. The CCK modulation is a variant of M-ary Bi-orthogonal Shift Keying (MBOK) [24, 26] and uses 8-chip complex codes for transmission of data.

OFDM uses several sub-carriers to send the symbols in a parallel manner and used by 802.11 a/g. The use of this technique increases the symbol time to counter delay spread while achieving higher data rates. An adaptive scheme giving fewer bits to the bad sub-carriers and vice versa can be used to maximize the system performance.

The IEEE 802.11b uses DSSS for data rates of 1,2 Mbps and HR/DSSS with CCK modulation for higher data rates of 5.5 and 11 Mbps. The corresponding sections give us insight into the 802.11 PHY as specified in the standard [9, 25].

2.4.1 PPDU Frame

The PHY Protocol Data Units frame is responsible for the correct reception of data and contains all the synchronization information necessary. The IEEE 802.11b defines two types of header and preambles for compatibility with the different data rates. The Long Physical Layer Convergence Procedure (Long PLCP) is defined for the data rates of 1 and 2 Mbps DSSS specifications, while the Short Physical Layer Convergence Procedure (Short PLCP) is defined for higher data rates rendering itself useful in applications desiring maximum throughput. The PLCP Service Data Units (PSDU) contains data to be transmitted. The data is modulated with any of the four modulation schemes namely 1 Mbps DPSK/BPSK, 2 Mbps DQPSK/QPSK, 5.5 and 11 Mbps CCK. An optional modulation scheme, PBCC is also used [9]. The 802.11b modulation schemes are described in detail in the next chapter.

2.4.2 Long PLCP Header

The Long PLCP Header and Preamble are shown in Tables 2.2 and 2.3 respectively. When the Long PLCP is in use, the Header and Preamble are modulated by 1 Mbps Barker sequence. The transmit time for the long PLCP header and preamble is 192μs.

PLCP Preamble 144 or 72 bits	PLCP Header 48 bits	PSDU variable no. of bits

Table 2.1: Building Blocks of a PPDU Frame

Sync 128 bits	SFD 16 bits

Table 2.2: Long PLCP Preamble

Signal 8 bits	Service 8 bits	Length 16 bits	CRC 16 bits

Table 2.3: Long PLCP Header

Long CRC

The cyclic redundancy check (CCITT CRC-16 FCS) is a parity bit- based error detection scheme widely used in serial data transmission applications and is based on polynomial arithmetic. Suppose the bit stream to be transmitted 1101011011 has 10-bits, representing a 10-term polynomial $M(x)$ where

$$M(x) = x^9 + x^8 + x^6 + x^4 + x^3 + x^1 + 1. \tag{2.1}$$

To compute the CRC of a given data frame, another polynomial called the generator polynomial is used. The $G(x)$ should have a degree greater than zero and less than that of the polynomial $M(x)$. An essential requirement for $G(x)$ is a non-zero coefficient in the x^0 term. This results in many options for $G(x)$, and hence the $G(x)$ are standardized. The generator polynomial specified by the standard for CRC-16 is given as

$$G(x) = x^{16} + x^{12} + x^5 + 1. \tag{2.2}$$

In general n-bit CRC is calculated as

$$\text{CRC} = \text{rem}\left[M(x) \times \frac{x^n}{G(x)}\right]. \tag{2.3}$$

2.4.3 Short PLCP Header

The Short PLCP Preamble is as shown in the Table 2.4 and the Short PLCP header is same as the one defined earlier in Table 2.2 for the Long PLCP. When the short PLCP is used, the preamble is modulated with the 1 Mbps DPSK Barker sequence and the header is modulated with the 2 Mbps DQPSK Barker sequence. The short PSDU is modulated using either 2 Mbps DQPSK or 5.5 or 11 Mbps CCK. The transmit time for the short header and preamble is $96\mu s$.

Sync	SFD
56 bits	16 bits

Table 2.4: Short PLCP Preamble

The various building blocks of the Long and Short header and preamble are described in complete detail in the IEEE 802.11b standard [9, 25] and are not implemented in our simulations. However,the effect of reducing the actual data throughput due to the presence of header and preamble has been considered.

2.5 IEEE 802.11b MAC

The Medium Access Control sublayer controls the transmissions between the data packets while avoiding collisions between them. The sections below give us detailed description of the IEEE MAC as specified in the standard [9, 25].

2.5.1 MAC Layer Packet Structure

Table 2.5 shows the format of the packets passed from the MAC layer to the PHY layer. Sometimes it becomes necessary to identify the address of the access point used by the transmitter and the receiver. For this purpose, four address fields are needed. This becomes

useful in a scenario when two WLAN users are sending packets to one another using different access points. The MAC addresses of both the clients and the access points will be present in the four address fields.

Frame Control 2 bytes	Duration and ID 2 bytes	Addr. 1 6 bytes	Addr. 2 6 bytes	Addr. 3 6 bytes	Sequence Control 2 bytes	Addr. 4 6 bytes	Frame Body 0-2350 bytes	FCS 4 bytes

Table 2.5: MAC Layer Packet Structure

2.5.2 Access Control

Since the 802.11 Wireless LAN clients transmit and receive on the same channel, the standard needs to define ways for transmission for the clients. The IEEE standard defines several multiple access mechanisms for this purpose. The Distributed Co-Ordination Function (DCF) uses the Carrier Sense Multiple Access Collision Avoidance (CSMA/CA) for contented access to the wireless networks and the Point Co-Ordination Function (PCF) for un-contended access to the wireless media via a Point Coordinator residing in the access point. In addition, the DCF also defines an optional Request-To-Send/Clear-To-Send (RTS/CTS) mechanism.

Abbreviation	**Meaning**
SIFS	Short Inter frame Spacing
PIFS	Point Coordination Function (PCF) Inter frame Spacing
DIFS	Distributed Coordination Function (DCF) Inter frame Spacing
EIFS	Extended Inter frame Spacing

Table 2.6: Different Frame Spacings

The DCF using CSMA/CA is more common because it shares the radio channel in a fair manner as opposed to the PCF which allocates a part of the radio channel bandwidth to some hosts. A "collision" takes place due to the simultaneous transmission or time-overlapping of two or more packets in a channel. Such a collision detection is not possible in wireless LANs.

Hence the IEEE 802.11 standard defines waiting periods as explained in Table 2.6 designed to avoid collisions between multiple users. This allows deferred access to multiple users to share the wireless channel.

2.5.3 CSMA/CA Operation

According to the CSMA/CA [27] principle, a transmitting node senses the channel and waits for a DIFS time period and then transmits in the free medium. The receiving node sends an ACK after a brief SIFS upon the correct reception of the transmitted packet. Collision is assumed to have occurred when the ACK frame is not received by the sending host. The host makes another attempt to send the packet when it senses the free channel for a period of time equivalent to a DIFS.

2.5.4 Hidden Node Problem

Before transmitting the packet, a node sends out a Ready-To-Send (RTS) packet containing information about the packet length. The receiving node responds with a Clear- To-Send (CTS) packet. The transmitting node sends the packet after this handshaking and awaits an ACK from the receiving node. To ensure the successful integrity of the packet, a CRC (cyclic redundancy check) is used. The hidden node problem is avoided by this handshaking as shown in Figure 2.4 .

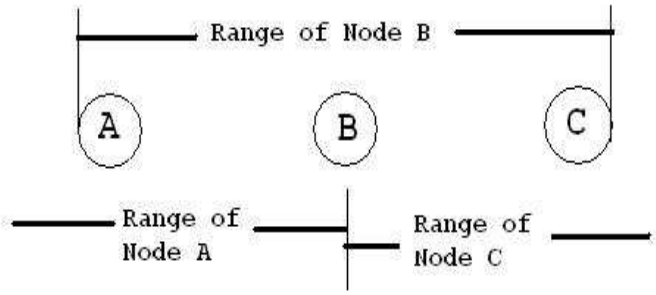

Figure 2.4: Hidden Node Problem reproduced from [2]

The hidden node problem [2] occurs when node B can hear both nodes A and C but A

and C cannot hear each other. Consider a situation where node C is transmitting data to node B, and node A and B want to start data transmission. In such a scenario, when node A sends its RTS packet to node B, it will not get any response from node B, thus avoiding the hidden node problem.

2.6 Conclusions

This chapter gives us the required information on the IEEE 802.11b PHY and MAC layers. However, this description is just a brief summary of the actual standard. We would recommend reading the actual standard [9, 25] for a broader perspective on the PHY and MAC layers. In the next chapter, we discuss the modulation schemes used in the 802.11b with performance results in AWGN and flat fading channels.

Chapter 3

Modulation schemes for the IEEE 802.11b Wireless LAN

3.1 Introduction

The IEEE 802.11b standard provides for three variations of the PHY namely; DSSS, FHSS and IR. The DSSS PHY option has a significant market presence and was designed specifically to operate in the 2.4 GHz ISM band in accordance with the FCC regulations. The worldwide allocations for the unlicensed operation of the ISM band are as summarized in the Table 3.1.

Region	**Allocated Spectrum**
US	2.4000 - 2.4835 GHz
Europe	2.4000 - 2.4835 GHz
Japan	2.4710 - 2.4970 GHz
France	2.4465 - 2.4835 GHz
Spain	2.4450 - 2.4750 GHz

Table 3.1: Global Spectrum Allocation at 2.4 GHz

The IEEE 802.11b technology transmitter implements various modulation modes for every transmission rate namely; DPSK for 1Mbps, DQPSK for 2 Mbps, and CCK for the higher data rates of 5.5 Mbps and 11 Mbps [28, 4, 29]. In the 802.11b frame, the data packets can be configured for DPSK, DQPSK or CCK while keeping DPSK as the transmission

mechanism for the header and the preamble.The type of modulation is indicated by the signal field in the packet header.

3.2 Advantages of Direct Sequence Spread Spectrum:

The DSSS PHY spreads the data using an 11-bit PN code called Barker Sequence before transmission. Thus each data bit to be transmitted is modulated by the 11-bit sequence. This results in the spreading of the signal over a much wider bandwidth as shown in the Figure 3.1 below.

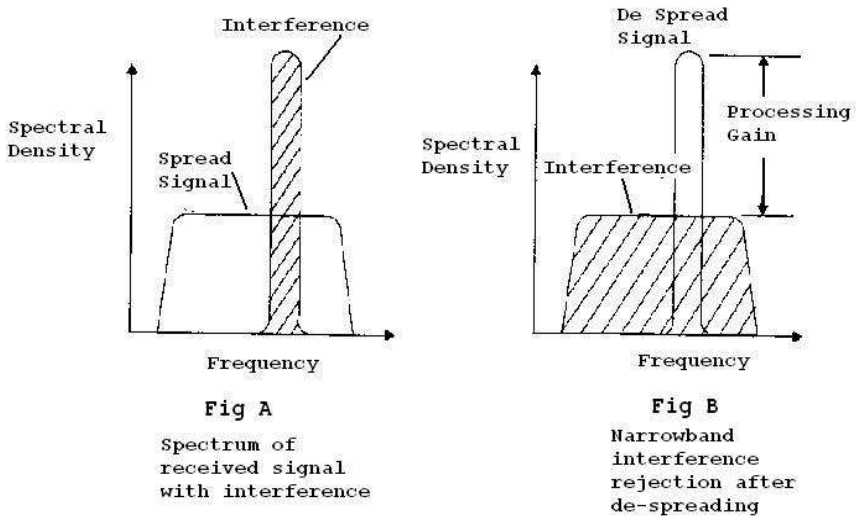

Figure 3.1: Use of DSSS in rejecting narrow band interference as reproduced from [3]

The DSSS spread signal transmitted over the channel is likely to be corrupted by narrowband interference sources similar to the one shown in the figure above. At the receiver the signal is subjected to de-spreading to get back the original data. As seen from Figure 3.1 B, the de-spreading actually spreads the narrowband interference over the entire signal bandwidth, while returning the actual information bearing signal to its original narrowband form. Thus, the spreading/de-spreading operation attempts to cancel out the harmful effects of the narrowband interference.

3.3 Spread Spectrum Modulation

Spread Spectrum [30] is employed in IEEE 802.11b to reduce the interference problem due to other systems operating in the same 2.4 GHz ISM band. The transmitted energy is thus spread over a wider amount of RF spectrum than normal and hence the name "spread spectrum". The binary data is multiplied (X-ORed) with a pseudorandom (PN) binary sequence to give rise to the spreading of the signal by a ratio of 11:1 as shown in Figure 3.2. DPSK and DQPSK use short and unique 11-chip Barker sequence with good autocorrelation properties as the PN code.

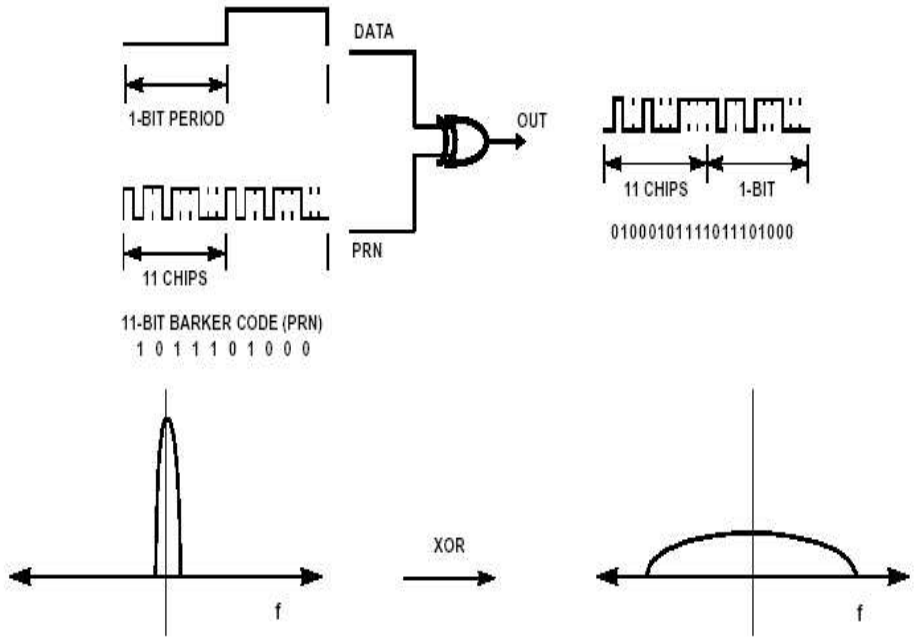

Figure 3.2: DSSS Spreading as reproduced from [4]

On reception, the received signal is demodulated to recover the binary stream.The bit decisions are made by correlating the recovered bit stream with the same 11-chip Barker sequence, restoring the original bandwidth and peak power as shown in Figure 3.3. The correlation process assumes significance from the fact that it reduces the level of narrow-band interference by a ratio of 11:1.

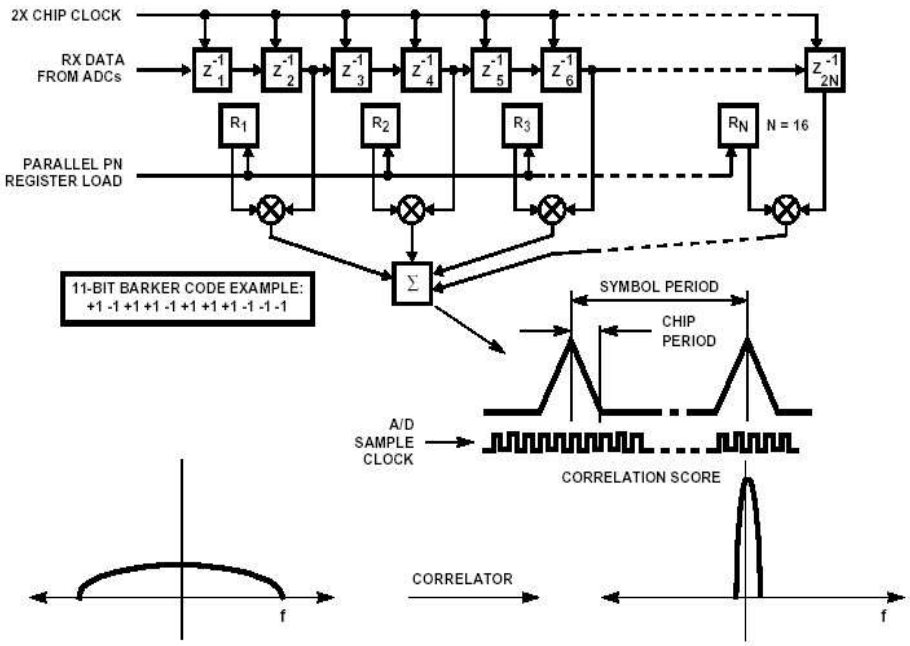

Figure 3.3: DSSS De-Spreading [4]

3.4 DPSK and DQPSK Modulations

3.4.1 Representation of Signals

DPSK and DQPSK is better explained with a brief introduction of the standard (coherent) phase shift keying (PSK). The signals in PSK can be written as

$$\begin{aligned} s_m(t) &= g(t)\cos\left[2\pi f_c t + \frac{2\pi}{M}(m-1)\right] \\ &= g(t)\cos\left[\frac{2\pi}{M}(m-1)\right]\cos(2\pi f_c t) - g(t)\sin\left[\frac{2\pi}{M}(m-1)\right]\sin(2\pi f_c t), \end{aligned} \tag{3.1}$$

where $g(t)$ is the signal pulse shape and $m = 1, 2, .., M$ represents the possible carrier phases conveying the transmitted information. BPSK is represented by $M = 2$ and QPSK is represented by $M = 4$. Figure 3.4 shows the signal space representation of the PSK signals.

DPSK differs from normal PSK in the symbol phase assignment. In DPSK, the difference between current and previous phase is detected indicating the change in symbol. For example the bit 1 may cause a phase shift of π while a 0 may cause no change in phase. The phase of every symbol is compared with the previous symbol to check for any phase changes. The bit 1 is detected for a phase change and likewise 0 is detected for no change in phase. DPSK

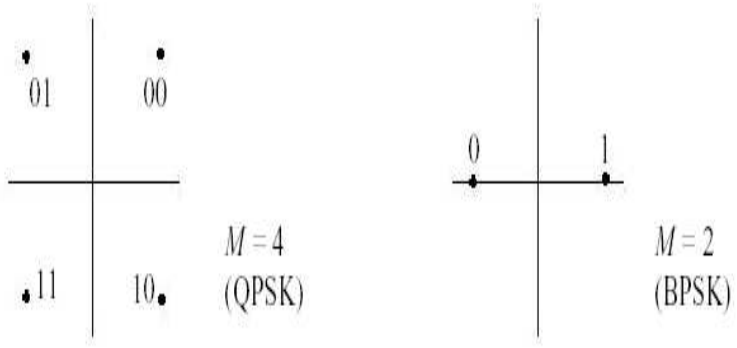

Figure 3.4: Signal Space Representation of PSK signals

is employed in the IEEE 802.11b system due to simplicity of the receiver design. This is because, differential modulation uses differentially coherent detection, eliminating the need for carrier phase estimation. The use of non-coherent detection simplifies the receiver design.

The bit error probability for differentially detected DPSK in an AWGN channel is given as [24]

$$P_e = \frac{1}{2}\exp\left(-\frac{E_b}{N_0}\right), \tag{3.2}$$

where the ratio of E_b to N_0 is defined as the normalized signal to noise ratio (SNR) in the AWGN channel.

For DQPSK, $M = 4$ and hence the bit error probability can be derived as [24]

$$P_e = Q_1(a,b) - \frac{1}{2}I_o(a,b)\exp\left(-\frac{1}{2}(a^2+b^2)\right), \tag{3.3}$$

where $Q_1(a,b)$ is the Marcum Q function, $I_o(a,b)$ is the modified Bessel function of zero order, and a and b are parameters defined as

$$a = \sqrt{\frac{2E_b}{N_0}\left(1-\sqrt{\frac{1}{2}}\right)} \quad \text{and} \quad b = \sqrt{\frac{2E_b}{N_0}\left(1+\sqrt{\frac{1}{2}}\right)}. \tag{3.4}$$

The data rate reached for the DPSK modulation scheme is about 1 Mbps, whereas with the DQPSK modulation a data rate of 2 Mbps is achieved.

3.4.2 Performance in an AWGN Channel

The bit error probabilities of DPSK and DQPSK versus signal-to-noise ratio operating in the AWGN channel are simulated and can be shown in Figure 3.5

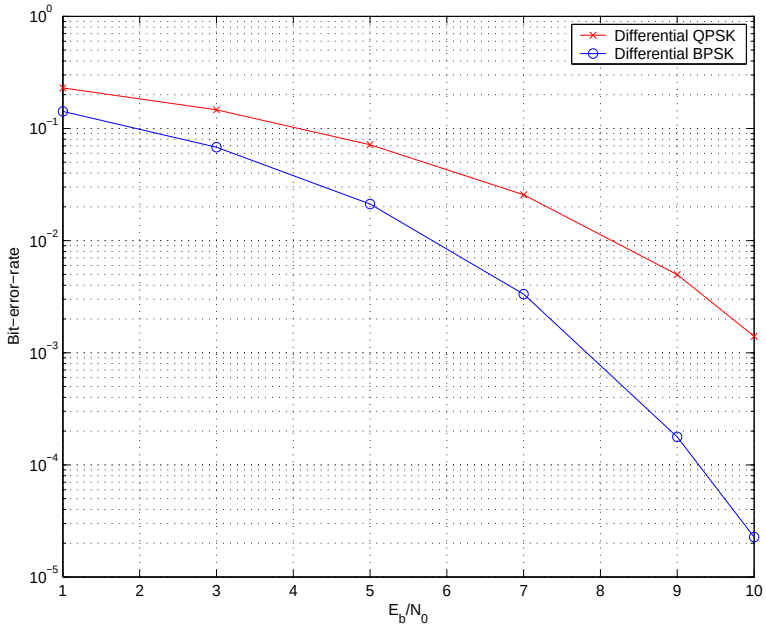

Figure 3.5: Bit Error Rate (BER) performance of DPSK and DQPSK in AWGN

3.5 CCK Modulation

3.5.1 Introduction

CCK can be described as a variant of M-ary Bi-Orthogonal Keying (MBOK) [26, 1] using codes having complex symbol structures. CCK uses the existing 802.11 1 and 2 Mbps DSSS channelization scheme for multi-channel operation in the 2.4 GHz ISM band [31, 26]. The spreading allows for 3 channels in the 2.4 to 2.483 GHz ISM band. CCK uses a complex set of Walsh/Hadamard functions known as Complementary Codes, having properties similar to Walsh functions but complex in nature (i.e. more than two phases while maintaining orthogonality). CCK modulation is based on complementary codes and employs an 8−chip spreading code.

3.5.2 Representation of a Single Signal

A signal in CCK modulation for the 11 Mbps scheme starts as an 8-bit data word, $d = d_7, d_6, d_5, ..., d_0$, and is converted to a complex vector using the DQPSK encoding table and formulas as shown below.

Bits	Phase Parameter
(d_1, d_0)	ψ_1
(d_3, d_2)	ψ_2
(d_5, d_4)	ψ_3
(d_7, d_6)	ψ_4

Table 3.2: Phase Assignment

Bits $[d_{i+1}, d_i]$	Phase
00	0
01	π
10	$\frac{\pi}{2}$
11	$\frac{3\pi}{2}$

Table 3.3: DQPSK encoding table

The modulation results in the code word $c = [c_0, c_1, c_2, c_3, c_4, c_5, c_6, c_7]$ where

$$\begin{aligned} \boldsymbol{c} = \big[& e^{j(\psi_1+\psi_2+\psi_3+\psi_4)}, e^{j(\psi_1+\psi_3+\psi_4)}, e^{j(\psi_1+\psi_2+\psi_4)} \ldots \\ & e^{-j(\psi_1+\psi_4)}, e^{j(\psi_1+\psi_2+\psi_3)}, e^{j(\psi_1+\psi_3)}, e^{-j(\psi_1+\psi_2)}, e^{j(\psi_1)} \big]. \end{aligned} \tag{3.5}$$

The 5.5 Mbps CCK scheme is encoded in a similar manner, except that we have 4 bits encoded in a single symbol i.e. $d = [d_3, d_2, d_1, d_0]$ instead of 8. The values of the phases $[\psi_1 ... \psi_4]$ are then calculated in a different manner. The first two bits $[d_1 \;\; d_0]$ are used to calculate the phase ψ_1 as before and phase $\psi_3 = 0$. The remaining phases are calculated as $\psi_2 = (d_2) * \pi + \pi/2$ and $\psi_4 = (d_3) * \pi$.

3.5.3 CCK Modulator and Demodulator

The CCK codeword c is transmitted over the noisy AWGN channel. CCK signals can be demodulated by using Fast Walsh Transform techniques or the Maximum Likelihood method as is described here. Since we have 8 bits in a codeword, the total number of possible codeword combinations is 256. The 11 Mbps ML demodulator stores all the 256 possible codewords in a look-up table. The received codeword $r = c + e$ is then compared

against all the possible codewords using a Euclidean distance measure to estimate the closest possible codeword.

3.5.4 Performance in an AWGN Channel

The CCK modulation for 11 Mbps can also be considered as an extended (8,4) quartenary Hamming code capable of correcting one symbol error per codeword [31]. The performance of a CCK signal in an AWGN environment is better than uncoded QPSK modulation as shown in the Figure 3.6. As expected, the 5.5 Mbps CCK signal performs marginally better than the 11 Mbps signal.

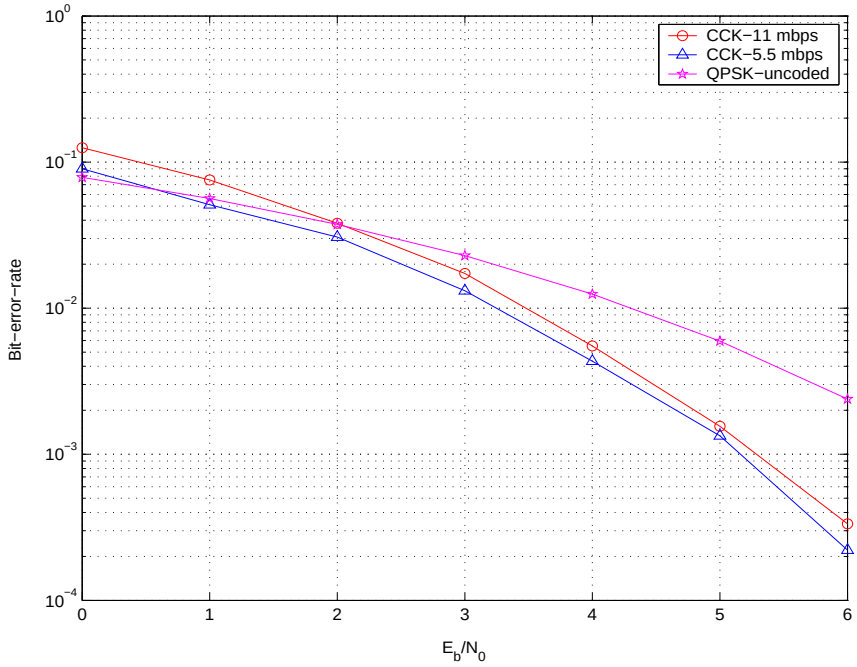

Figure 3.6: Bit Error Probability (BER) of CCK modulation - AWGN channel

The improvement in performance over uncoded QPSK is due to the coding properties of the spreading code which correlates several bits together to generate the symbols. The 5.5 Mbps signal starts as a group of four data bits and is mapped into eight DQPSK symbols giving a code rate of 1/4. Similarly the 11 Mbps eight data bits are mapped to eight DQPSK symbols thus giving a code rate of 1/2. The union bound on the codeword error probability for the 11 Mbps CCK signal as given by [31] is $P_c = Q\sqrt{(2E_b/N_0)}$ and the bit error rate

BER is approximately $(1/2)P_c$.

3.6 Performance of 802.11b in a Slow Flat Fading Environment

The probability of error in a slow fading channel can be found out by averaging the instantaneous probability of error of the modulation scheme in AWGN channels over the range of signal strength due to fading. The average probability of error in a fading channel can thus be obtained by averaging the probability of error in AWGN channels over the probability density function (PDF) of the fading channel. That is,

$$P_e = \int_0^\infty P_e(X)p(X)dX, \tag{3.6}$$

where $P_e(X)$ is the probability of error for any modulation scheme at a specific Signal-to-Noise ratio (SNR) X and $p(X)$ is the PDF of X as a result of the channel.

The instantaneous SNR X is given as $X = \alpha^2 E_b/N_0$, where E_b represents the average energy per bit and N_0 is the noise power spectral density in the AWGN channel. The instantaneous power values of the fading channel with respect to the non-fading SNR is represented by α^2. For a unity gain fading channel, we can assume $E\{|\alpha|^2\} = 1$. Thus $P_e(X)$ can be assumed to be the conditional probability of error rate due to fading for a given SNR and $p(X)$ can be viewed as the instantaneous SNR in a fading channel.

In a Rayleigh fading channel, the fading coefficient α follows a Rayleigh distribution; hence X will have a chi-square distribution with two degrees of freedom. Thus

$$p(X) = \frac{1}{\Gamma}\exp\left(\frac{-X}{\Gamma}\right) \qquad X \geq 0, \tag{3.7}$$

where $\Gamma = \frac{E_b}{N_0}\alpha^2$ is the average SNR. The Γ corresponds to the average signal-to-nose ratio of the channel. By using Equation (3.7) and the probability of error for a modulation scheme in an AWGN channel, we can evaluate the probability of error in a flat fading channel.

Thus, the average probability of error (BER) for 1 Mbps DPSK can be derived as

$$P_{e,DPSK} = \frac{1}{2(1+\Gamma)}. \tag{3.8}$$

For higher values of E_b/N_0, i.e. larger X values, the probability of error equation can be simplified as

$$P_{e,DPSK} = \frac{1}{4\Gamma}. \tag{3.9}$$

3.7 Discrete Time Model for a Fading Channel

The channel between the transmitter and the receiver antennas can be modelled as

$$h = \alpha_n e^{j\theta_n} \tag{3.10}$$

with α_n being the Rayleigh distributed channel attenuation and θ_n the phase, uniformly distributed between $[0, 2\pi]$. The channel is assumed to be quasi-static flat-fading channel constant over the duration of an entire packet

For a flat-fading channel, the continuous time signal can be represented as

$$r(t) = h_1 s_{wlan}(t) + w(t) \tag{3.11}$$

where $s_{wlan}(t)$ is the WLAN signal, $w(t)$ is the Additive White Gaussian Noise (AWGN) with channel attenuation $h_1 = \alpha_1 e^{j\theta_1}$.

At the receiver, the continuous time signal is subjected to matched filtering and a detection process. Hence, we can represent this continuous time signal in discrete-time vector form as

$$\boldsymbol{r} = h_1 \boldsymbol{s_{wlan}} + \boldsymbol{w} \tag{3.12}$$

where $\boldsymbol{r} = [r_1, r_2, ..., r_N]^T$, $\boldsymbol{s_{wlan}} = [s_1, s_2, ..., s_N]^T$ and $\boldsymbol{w} = [w_1, w_2, ..., w_N]^T$, with N being the length of a WLAN packet, s_{wlan_i} being the complex WLAN modulated symbols and w_i being the complex random noise. Also, $r_i = \int_{(i-1)T}^{iT} r(t)\ \psi(t - iT)\, dt$ with $\psi(t)$ being the pulse shape.

The discrete time model model thus derived is the result of matched filtering the received signal, which generates sufficient statistics for a discrete-time representation. The discrete-time model obtained from the continuous time representation is described in detail in Appendix B and is used for simplifying the signal detection process.

3.7.1 Bit Error Rate - Single Antenna Receiver

The WLAN receiver with a single antenna can be modelled as shown in Equation (5.7). Assuming channel knowledge at the receiver, we can estimate the received signal as

$$\begin{aligned} \hat{\boldsymbol{s}}_{\mathbf{wlan}} &= {h_1}^* \boldsymbol{r} = |h_1|^2 \boldsymbol{s_{wlan}} + {h_1}^* \boldsymbol{w} \\ &= {\alpha_1}^2 \boldsymbol{s_{wlan}} + \tilde{\boldsymbol{w}}. \end{aligned} \tag{3.13}$$

The Figure 3.7 shows the performance in a fading channel. As seen, the bit error rate of the CCK signal is superior to uncoded BPSK.

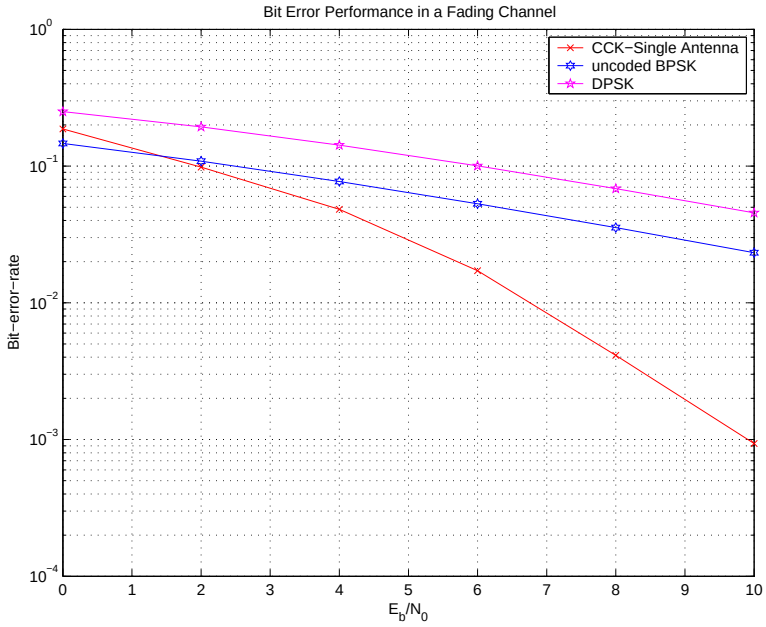

Figure 3.7: BER of CCK 11Mbps in a Fading Channel - Single Antenna Receiver

As expected, the performance of the 11 Mbps CCK system is better than uncoded QPSK. The performance as discussed before over uncoded QPSK is due to the coding properties of the spreading code which correlates several bits together to generate the symbols.

3.8 Conclusions

In this chapter, we focussed on simulation of the modulation schemes used in 802.11b, with performance results for AWGN and flat-fading channels. We will use these simulations

later in the report to present a throughput simulator with optimized packet sizes. In the next chapter, we focus on the Bluetooth system and simulate the 1 Mbps GFSK modulation used in Bluetooth.

Chapter 4

Overview of Bluetooth

4.1 Introduction

The idea of Bluetooth originated from the need to use short-range wireless links for on-demand device connectivity between any two devices. Bluetooth was a result of a consortium between IBM, Intel, Nokia, Toshiba and Ericsson, created towards providing low cost, low power, single chip wireless hand-held connectivity. Technically speaking, "Bluetooth is a short-range, low-power radio link (0-10m) between two devices operating in the unlicensed 2.4-GHz industrial scientific and medical (ISM) band" [8, 32, 5, 33].

4.2 Piconets and Scatternets

In the ISM band, Bluetooth uses Frequency Hopping Spread Spectrum (FHSS) at a rate of 1600 hops/sec allowing multiple channels to co-exist in the same band without any interference issues. A set of Bluetooth units sharing the same channel constitute a piconet. The central device acts as the master of the piconet, with the other units as slaves. Ideally, a master can serve up to seven slaves. Communication between multiple piconets is possible in Bluetooth due to a structure called as a scatternet as shown in Figure 4.1. For a piconet, the frequency hopping sequence is decided by the master, with all the slaves synchronized to it.

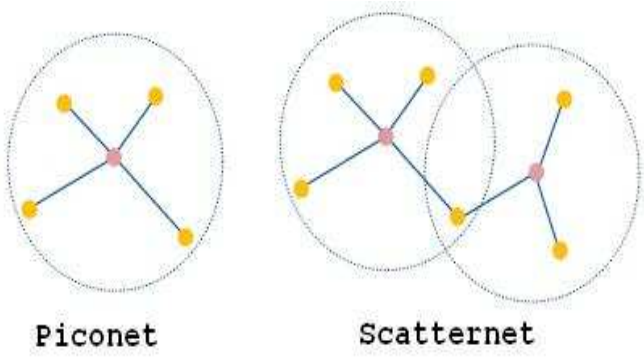

Figure 4.1: Piconet and Scatternet as reproduced from [5]

4.3 Channel and Time Slots

In Spain, France and Japan, the 2.4 GHz ISM band allocates a smaller frequency spectrum compared to the 83.5 MHz spectrum allocation in USA and most of the European countries. Thus, 79 channels with a spacing of 1 MHz are defined for US and Europe as opposed to 23 1-MHz-spaced channels defined for Japan, Spain and France. Each time slot on a channel corresponds to an RF hop frequency. Each time slot in a channel is $625\mu s$ in length. Interference free data communication between two Bluetooth devices is achieved by ensuring that the communicating Bluetooth devices stay on the same hop frequency for a single time slot before next data transmission. The RF hop frequency for a packet is derived from the current Bluetooth clock value and the first slot of the packet for a multi-slot packet.

4.4 Radio Specification

The radio specification defines the transmitter and receiver characteristics, frequency bands, modulation characteristics and receiver sensitivity. The output power of Bluetooth devices ranges from 1mW to 10mW. Modulation is Gaussian frequency shift keying (GFSK) with BT_b=0.5, modulation index between 0.28 and 0.35 and symbol timing better than 20 parts per milion. Also, the zero crossing error should be less than 1/8 of symbol period.

4.5 Gaussian Frequency Shift Keying

The modulation is GFSK (Gaussian Frequency Shift Keying) with BT_b= 0.5. The modulation index m should be between 0.28 and 0.35. A value of 0.32 for m was selected for this project. In GFSK, a binary one is represented by a positive frequency deviation while a negative frequency deviation represents a binary zero. The zero crossing error, defined as the time difference between the ideal symbol period and the measured crossing time is less than ± 1/8 of a symbol period. Thus, a Bluetooth modulated interfering signal is defined as:

- Modulation: Gaussian Frequency Shift Keying.
- Modulation index m : 0.32
- BT_b : 0.5
- Frequency accuracy better than ±1 ppm .
- Bit Rate: 1 Mbps.

4.5.1 Transmitter

In GFSK transmitter, a binary sequence $\{a_i\}$, $a_i \in (+1, -1)$ is converted into NRZ pulse of duration T_b and then shaped by a unity-gain Gaussian shaping filter with a bandwidth B, where T_b is the symbol time interval and BT_b=0.5 [8, 34]. The baseband signal is represented by $s(t)$ [34, 35, 36]

$$s(t) = \sqrt{\frac{2E_b}{T_b}} \exp\left(j\theta(t)\right) \quad \text{and} \quad \theta(t) = 2\pi m \sum\nolimits_i a_i \int_{-\infty}^{t-iT_b} g(u)du \tag{4.1}$$

where E_b is the bit energy and $\theta(t)$ is the phase of the modulated signal, m is the modulation index (0.32 for Bluetooth) and $g(t)$ is the Gaussian shaping pulse.

The Gaussian filter transfer function $h_{trans}(t)$ assumes the form

$$h_{trans}(t) = \frac{1}{\sqrt{2\pi}\sigma T_b} \exp\left(\frac{-t^2}{2\sigma^2 {T_b}^2}\right) \tag{4.2}$$

where $\sigma = \frac{\sqrt{\ln(2)}}{2\pi B_T}$ and BT_b =0.5 for Bluetooth. The impulse response of the Gaussian

pre-filter can then be given as

$$g(t) = \frac{1}{2T_b}\left(Q\left[2\pi B_T \frac{t - T_b/2}{T_b\sqrt{\ln(2)}}\right] - Q\left[2\pi B_T \frac{t + T_b/2}{T_b\sqrt{\ln(2)}}\right]\right). \tag{4.3}$$

The basic block diagram for our transmitter-receiver is as shown in Figure 4.2. The channel for this system is considered to be an Additive White Gaussian Noise (AWGN) channel.

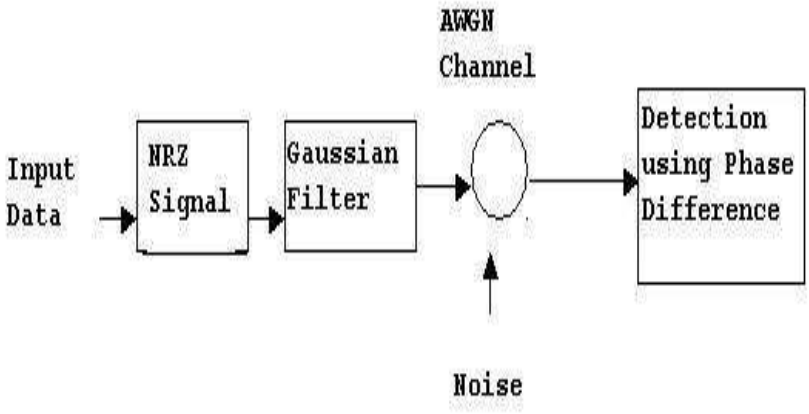

Figure 4.2: The GFSK Transmitter Receiver System

4.5.2 Receiver

GFSK detection can be implemented with a variety of receivers like Viterbi Decoder [35] or LDI receiver [35, 36]. These models provide satisfactory performance in the presence of multipath fading and channel coding. At baseband, the simplest implementation of GFSK demodulation is based on the fact that, in a binary decision making scheme, the sign of the phase difference between the sampling instants gives the final decision of the transmitted data bit [34]. The receiver for GFSK thus boils down to calculating the phase differences for a symbol and comparing them with the originally transmitted data bits. Thus,

$$\theta_x(k) = \theta_x(t_k + 1) - \theta_x(t_k). \tag{4.4}$$

with k being the time instant.The phase difference [34] contains the signal $\{a_i\}$ and the inter-symbol interference (ISI) term. Figure 4.3 gives the performance of the Bluetooth system in an AWGN channel for a baseband implementation.

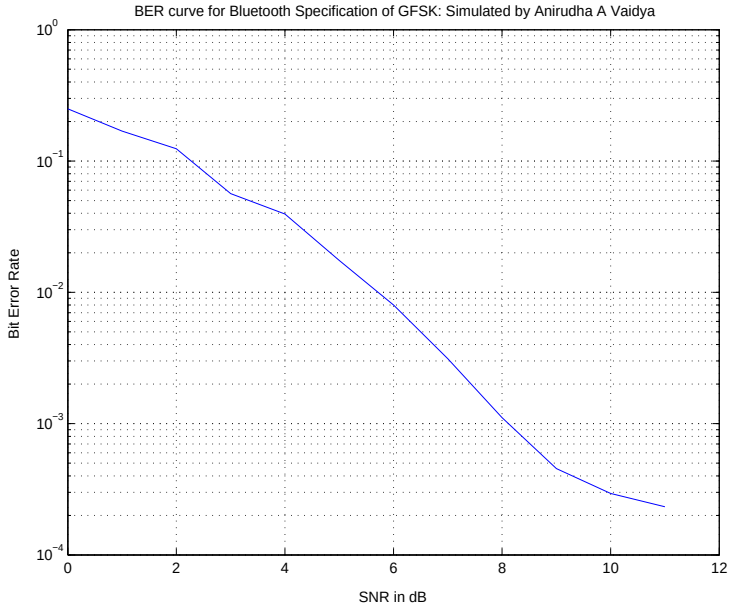

Figure 4.3: Bit Error Probability of GFSK modulation : AWGN channel

4.6 Conclusions

In this chapter, we introduced the Bluetooth system and presented simulation results for GFSK modulation. The GFSK modulated signal will be the interfering signal for our interference model to be presented in the next chapter.

Chapter 5

802.11b Interference with Bluetooth: The PHY Simulator

5.1 Introduction

IEEE 802.11b and Bluetooth both occupy the 2.4 GHz ISM frequency band, paving the way for interference issues between them. IEEE 802.11b WLAN occupies a bandwidth of 22 MHz for a single channel, where as Bluetooth with its FHSS scheme uses 79 MHz of the available bandwidth, thus resulting in a certain collision probability of a Bluetooth packet with a WLAN packet. The Bluetooth applications transmit signals with a transmit power of 1mW which is significantly lower than the transmit power of 100 mW of the 802.11b WLAN system. The simulations performed here take into account the relative power levels of the Bluetooth and the 802.11b signals.

The quality of service (QoS) of a communication link is given by its signal-to-noise ratio (SNR) defined as SNR $= \frac{E_b}{N_0}$. For the bit-error simulations with the interference issues related to Bluetooth, the Signal-to-Interference ratio (SIR) is defined as

$$\text{SIR} = \frac{E_w}{E_I} \tag{5.1}$$

where E_w is the average bit energy of the WLAN signal and E_I is the average bit energy of the Bluetooth signal.

The Bluetooth and 802.11b packets have to overlap in frequency and time for a collision between them as shown in Figure 5.1 below.

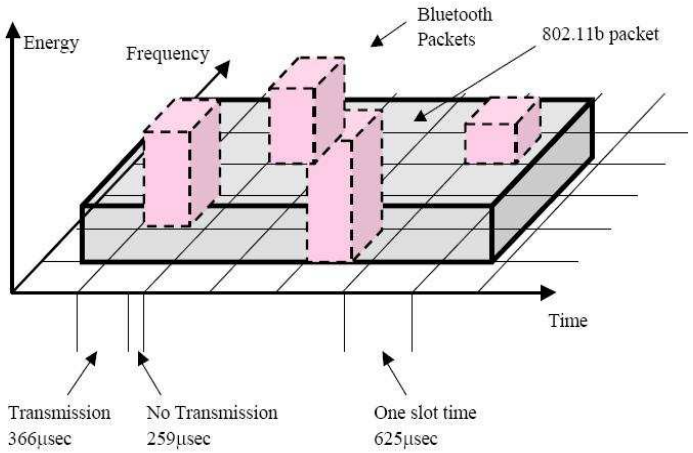

Figure 5.1: Overlap of Bluetooth packets with an 802.11b packet in frequency and time as reproduced from [1]

The Bluetooth system transmits data in bursts of $625\mu s$. For a Bluetooth burst of $625\mu s$, actual transmission of the signal occurs for $366\mu s$ followed by an idle time of $259\mu s$. In the interference model discussed here, we consider Bluetooth transmission using DM1/DH1 single slot packets. The frequency overlap probability P_o gives us the percentage of collision of the Bluetooth and 802.11b packets in the frequency domain. In these simulations the collision of Bluetooth with 802.11b packets is modelled as a random variable with a value less than P_o.

Let W_R be the bandwidth of the 802.11b received signal, W_T be the bandwidth of the Bluetooth interfering signal and N_c is the number of channels in which the the Bluetooth system hops. [37].

The frequency overlap probability can be derived as

$$P_o = W_R/(W_T \times N_c) = 22\text{MHz}/(1\text{MHz} \times 79) = 27.8\%. \tag{5.2}$$

5.2 Interference Model: The Physical Layer Simulator

This section describes the implementation of the IEEE 802.11b PHY layer with Bluetooth interference. This simulation does not implement the PHY Protocol Data Units frame (PPDU), which contains all the necessary information for synchronization. Thus the problem of synchronization is not considered in this simulation. The PHY layer for this model is

simulated at baseband. The block diagram of the PHY later simulation can be shown in Figure 5.2.

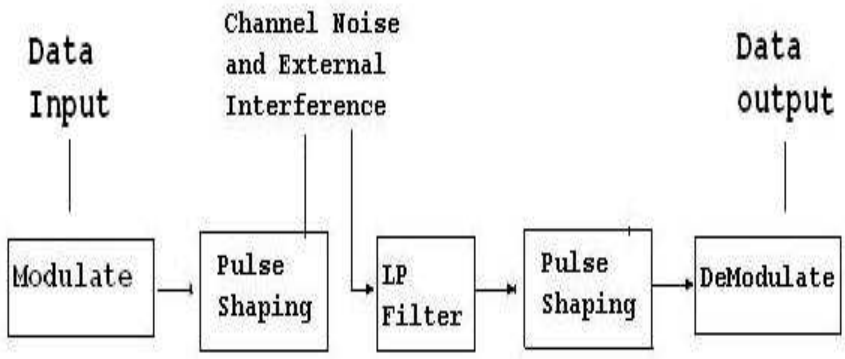

Figure 5.2: PHY layer simulation as reproduced from [2]

5.2.1 The 802.11b PHY Simulator

Randomly generated data bits are modulated and pulse shaped with a square-root-raised-cosine filter having a roll-off factor of 0.5 as shown in Figure 5.3.

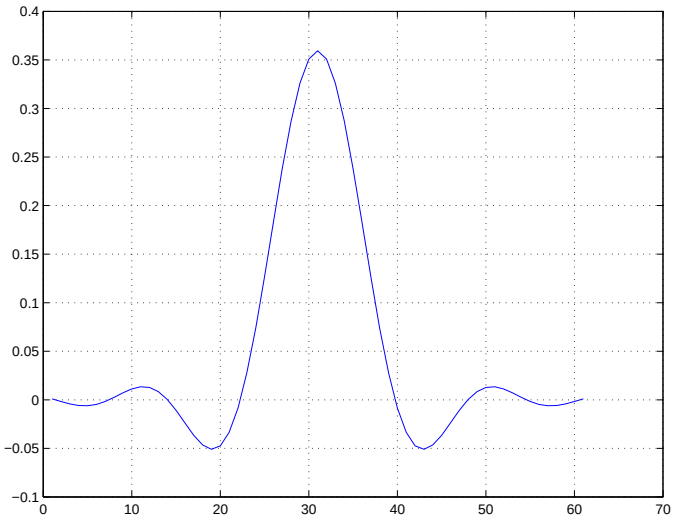

Figure 5.3: Raised Cosine Roll-off Filter Pulse Shape in the time domain

The signal thus generated is transmitted over the channel. The presence of Bluetooth interference and the channel gains corrupt the signal as it arrives at the receiver. At the receiver, the signal is subjected to low-pass filtering and pulse shaping by the square-root-raised-cosine filter. The filtered signal is then decoded and demodulated with the appropriate demodulators. The number of bits in error received gives us the Bit Error Rate (BER) of the system with Bluetooth interference. The following sections give us an account of the performance degradation in terms of the BER due to the presence of Bluetooth Interference. The number of packets received in error is given by the Packet Error Rate (PER). The PER increases as the packet size increases. The effect of using different packet sizes on the throughput of the system is considered in the latter part of the report.

5.2.2 802.11b WLAN Modulation

The modulation schemes used were DPSK and DQPSK with DHSS spreading. In these cases, an 11 Bit Barker sequence $[-1, -1, -1, 1, 1, 1, -1, 1, 1, -1, 1]$ was used for DSSS spreading. The effect of the spreading operation results in increasing the bandwidth of the transmitted 802.11b signal to 22 MHz. The BT signal occupies 1 MHz bandwidth and hops randomly using the 79 channels specified in the 83.5 MHz ISM band, thus acting as a narrowband interferer for the 802.11b signal. The 5.5 and 11 Mbps CCK modulations were also used in the simulations. The CCK signals were detected using the ML detector by comparing the received codeword against all the possible codewords stored in a lookup table.

5.3 Discrete time model for the AWGN channel

For an AWGN channel, the continuous time signal can be represented as

$$r(t) = s_{wlan}(t) + s_{bt}(t) + w(t) \tag{5.3}$$

where $s_{wlan}(t)$ is the WLAN signal, $s_{bt}(t)$ is the Bluetooth interferer and $w(t)$ is the Additive White Gaussian Noise (AWGN).

At the receiver, the continuous time signal is subjected to matched filtering and detection process. Hence, we can represent this continuous time signal in a discrete time vector form

as

$$\boldsymbol{r} = \boldsymbol{s_{wlan}} + \boldsymbol{s_{bt}} + \boldsymbol{w} \tag{5.4}$$

where $\boldsymbol{r} = [r_1, r_2, ..., r_N]^T$, $\boldsymbol{s_{wlan}} = [s_1, s_2, ..., s_N]^T$, $\boldsymbol{s_{bt}} = [b_1, b_2, ..., b_N]^T$ and $\boldsymbol{w} = [w_1, w_2, ..., w_N]^T$, with N being the length of a WLAN packet and s_{wlan_i} being the complex WLAN modulated symbols, s_{bt_i} being the complex GFSK modulated symbols, and w_i being the complex random noise. Also, $r_i = \int_{(i-1)T}^{iT} r(t)\ \psi(t - iT)\, dt$ with $\psi(t)$ being the pulse shape.

5.4 Performance in an AWGN Channel

This section demonstrates the performance of DPSK and CCK modulation schemes in the presence of a Bluetooth interferer. For an AWGN channel, the discrete-time received signal can be modelled as shown above in Equation (5.4).

This discrete-time model is the result of matched filtering the received signal, which generates sufficient statistics for a discrete time representation. The discrete-time model obtained from the continuous time representation is described in detail in Appendix A and is used for simplifying the signal detection process.

We assume that the Bluetooth interferer transmits packets using random FHSS in bursts of $625\mu s$ at a data rate of 1 Mbps. A single BT burst is transmitted as 625 bits of GFSK modulated signal. Thus for a frame of 1600 bits, we can have anywhere between 0 to 3 Bluetooth bursts.

The performance of 1 Mbps DPSK signal in the presence of a Bluetooth interferer is as shown in the Figure 5.4 below.

Similarly, the bit error performance of 11 Mbps CCK in the presence of a Bluetooth interferer is shown in Figure 5.5 below. The CCK performance gets closer to AWGN performance as the Signal to Interference Ratio (SIR) increases.

5.5 Discrete time model for a fading channel

As given earlier, the channel between the transmitter and the receiver antennas can be modelled as

$$h = \alpha_n e^{j\theta_n} \tag{5.5}$$

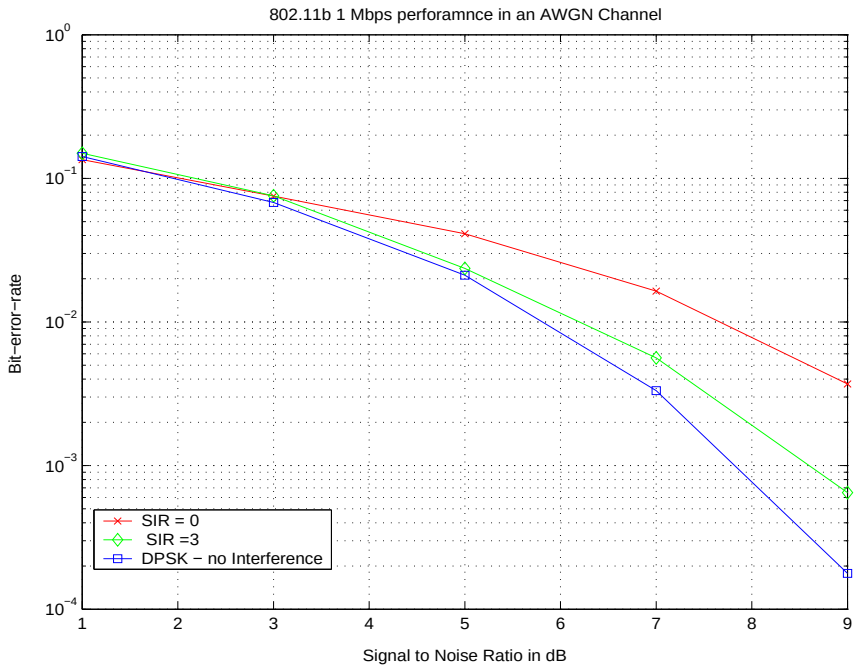

Figure 5.4: Bit Error Probability of DPSK with Bluetooth Interference

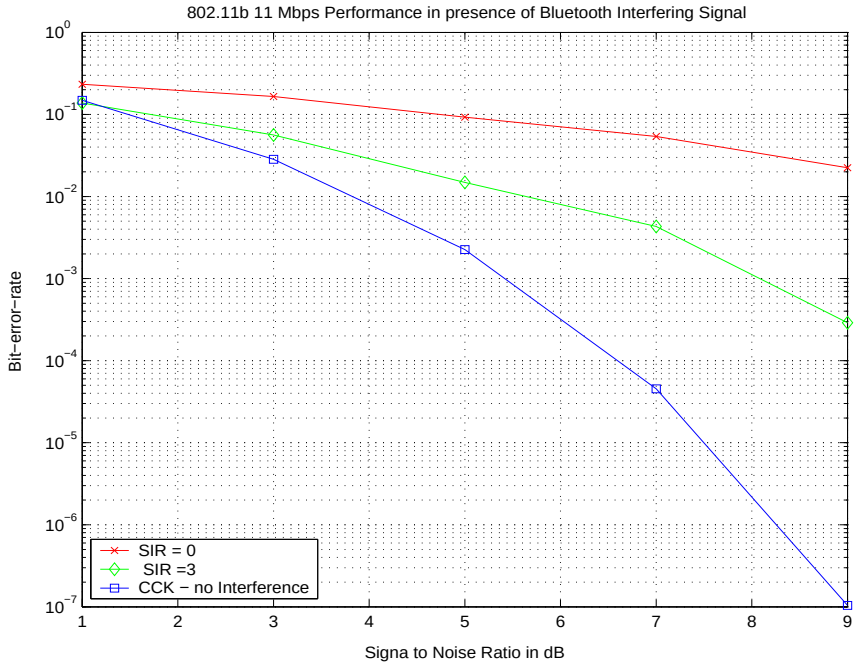

Figure 5.5: Bit Error Probability of 11 Mbps CCK with Bluetooth Interference

with α_n being the Rayleigh distributed channel attenuation and θ_n the phase, uniformly distributed between $[0, 2\pi]$. The channel is assumed to be time-invariant flat-fading channel

constant over the duration of an entire packet.

For a flat-fading channel, the continuous time signal can be represented as

$$r(t) = h_1 s_{wlan}(t) + h_2 s_{bt}(t) + w(t) \tag{5.6}$$

where $s_{wlan}(t)$ is the WLAN signal, $s_{bt}(t)$ is the Bluetooth interferer, $w(t)$ is the Additive White Gaussian Noise (AWGN) with channel attenuations as $h_1 = \alpha_1 e^{j\theta_1}$ and $h_2 = \alpha_2 e^{j\theta_2}$.

At the receiver, the continuous time signal is subjected to matched filtering and detection process. Hence, we can represent this continuous time signal in a discrete time vector form as

$$\boldsymbol{r} = h_1 \boldsymbol{s_{wlan}} + h_2 \boldsymbol{s_{bt}} + \boldsymbol{w} \tag{5.7}$$

where $\boldsymbol{r} = [r_1, r_2, ..., r_N]^T$, $\boldsymbol{s_{wlan}} = [s_1, s_2, ..., s_N]^T$, $\boldsymbol{s_{bt}} = [b_1, bt_2, ..., b_N]^T$ and $\boldsymbol{w} = [w_1, w_2, ..., w_N]^T$, with N being the length of a WLAN packet and s_{wlan_i} being the complex WLAN modulated symbols and w_i being the complex random noise. Also, $r_i = \int_{(i-1)T}^{iT} r(t)\ \psi(t - iT)\, dt$ with $\psi(t)$ being the pulse shape.

5.6 Performance in a Fading Channel

This section demonstrates the performance of DPSK modulation scheme in the presence of a Bluetooth interferer. For the flat-fading channel, the discrete-time received signal can be modelled as shown above in Equation (5.7).

Similar to the AWGN model, this model is the result of matched filtering the received signal, which generates sufficient statistics for a discrete time representation. The discrete-time model for the fading channel is obtained from the continuous time representation as described in the Appendix B, and is used for simplifying the signal detection process.

5.6.1 Single Antenna Receiver

The WLAN receiver with a single antenna can be modelled as shown in Equation (5.7). Assuming the channel knowledge at the receiver, we can estimate the received signal as

$$\begin{aligned} \hat{\boldsymbol{s}}_{\mathbf{wlan}} &= {h_1}^* \boldsymbol{r} \\ &= \underbrace{|h_1|^2}_{\alpha_1^2} \boldsymbol{s_{wlan}} + \underbrace{{h_1}^* h_2 \boldsymbol{s_{bt}}}_{\tilde{s_{bt}}} + \underbrace{{h_1}^* \boldsymbol{w}}_{\tilde{w}} \\ &= {\alpha_1}^2 \boldsymbol{s_{wlan}} + \tilde{\boldsymbol{s_{bt}}} + \tilde{\boldsymbol{w}}. \end{aligned} \tag{5.8}$$

The performance of 1 Mbps DPSK signal in the presence of a Bluetooth interferer is as shown in the Figure 5.6 below. The 1 Mbps system uses 11-chip DSSS spreading as specified in the standard. DSSS spreading increases the resistance of the system to a narrow band interferer such as Bluetooth. The 802.11b WLAN performance gets closer to the no interference case performance as the SIR increases.

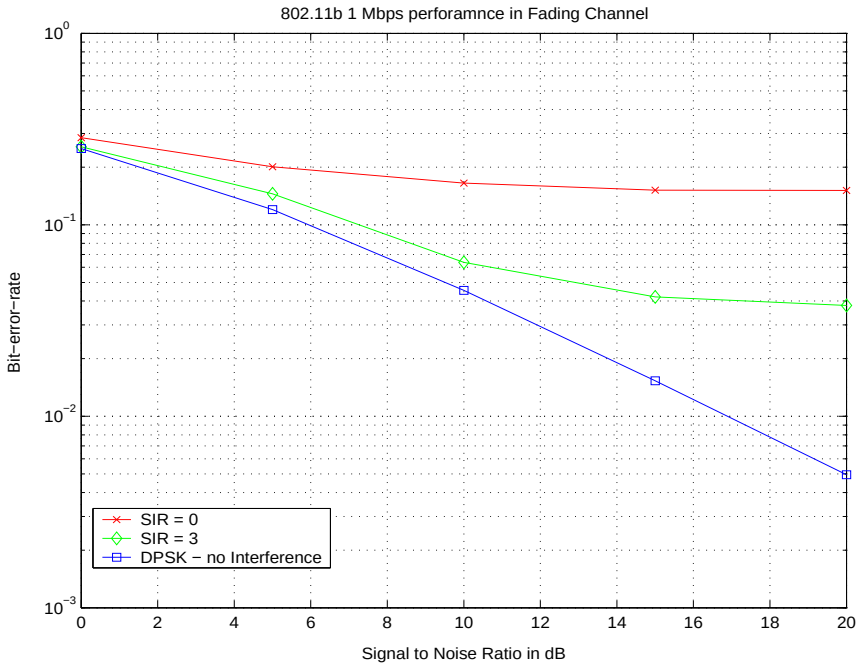

Figure 5.6: Bit Error Probability for DPSK: Single Antenna Receiver

5.7 Conclusions

In this chapter, we presented a model for the interference of a Bluetooth signal with an 802.11b signal, and presented results for the bit-error-rate of the 802.11b system. However, in an actual system implementation, the probability of packet error or packet error rate (PER) assumes greater significance. The packet error probability gives us a direct indication on the maximum throughput possible for the system. In the chapters to follow, we discuss the channel model for a typical wireless channel with large scale and small scale fading. The channel model is used to analyze the throughput of the 802.11b Wireless LAN. By defining suitable network topologies, we also analyze the performance of 802.11b in the presence of BT interferers. The optimum packet sizes obtained from this analysis are then finally used for actual throughput simulations in Chapter 10.

Chapter 6

Channel Characterization for Throughput Analysis

6.1 Introduction

In the mobile wireless channel, the transmission path from the transmitter to the receiver can vary from line-of-sight propagation to severely obstructed propagation. The wireless channels are extremely random and unpredictable, unlike the wired channels which are comparatively stationary. The wireless channel modelling is hence done in a statistical fashion, based on specific measurements. The loss in a wireless channel can be expressed as,

$$Channel(dB) = \underbrace{PL(dB) + X_\sigma}_{LargeScaleFading} + Y. \tag{6.1}$$

The first two terms represent the large scale fading loss and the last term represents the channel impairment due to small scale fading.

6.2 Large Scale Fading

6.2.1 Log-distance Path Loss Model

Based on the theoretical and measurement-based propagation models, we know that the received signal power decreases logarithmically with the distance. Thus the average large-scale path loss as a function of distance between the transmitter and the receiver can be

expressed as given in [3]

$$\overline{PL}(d) \propto \left(\frac{d}{d_0}\right)^n \tag{6.2}$$

or

$$\overline{PL}(d) = \overline{PL}(d_0) + 10n \log\left(\frac{d}{d_0}\right). \tag{6.3}$$

Here n is the path loss exponent, indicating the rate of increase of the path loss with the increasing distance d between the transmitter and the receiver, d_0 is the close-in reference distance determined from the measurements from the transmitter.

As shown from Table 6.1, the value of n depends on the propagation environments.

Environment	Path Loss Exponent, n
Free Space	2
Urban area cellular radio	2.7 to 3.5
shadowed urban cellular radio	3 to 5
In building line-of-sight	1.6 to 1.8
Obstructed in building	4 to 6
Obstructed in factories	2 to 3
Indoor Environments	2 to 4

Table 6.1: Path Loss Exponents for different environments as reproduced from [3]

The choice of the free space reference distance for the environment is important for modelling the system. Large cellular systems have 1 km as the reference distances whereas, the microcellular systems select reference distances in the range 1 m to 100 m.

The close-in reference distance path loss $PL(d_0)$ is given by the formula as follows

$$\overline{PL}(d_0) = 20 \log\left(\frac{4\pi d_0}{\lambda}\right). \tag{6.4}$$

With n=3.5 and the power of the 802.11b transmitter to be 100 mW or 20dBm, the path loss for 100 meters can be shown in Figure 6.1.

6.2.2 Log-normal Shadowing

The log-distance model in Equation (6.3) does not consider the varying surrounding environmental clusters and different T-R separations. Thus the measured values of the

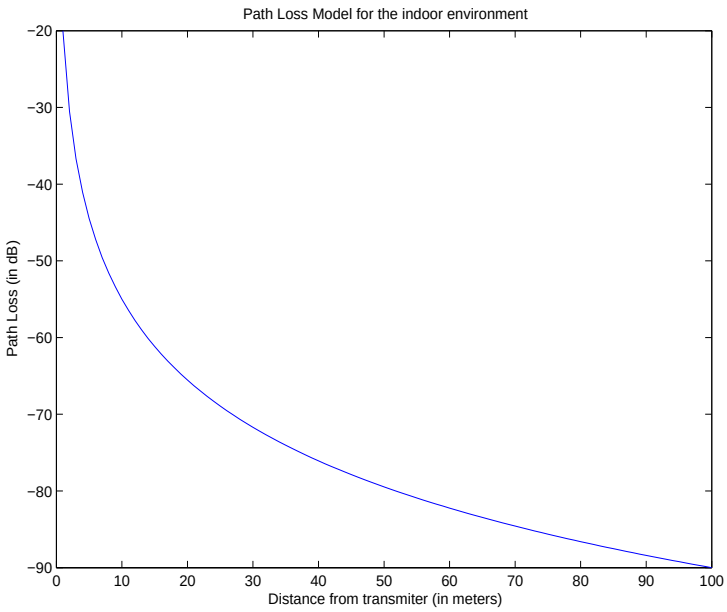

Figure 6.1: Path loss for the indoor environment

signals are vastly different from the average values as predicted by Equation (6.3). Past measurements have shown that the path loss $PL(d)$ at a location d to be random and log-normally distributed about the mean distance-dependant value [3]. Thus we have,

$$PL(d)[dB] = \overline{PL}(d) + X_\sigma = \overline{PL}(d_0) + 10n \log\left(\frac{d}{d_0}\right) + X_\sigma. \tag{6.5}$$

and also

$$P_r(d)[dBm] = P_t[dBm] - PL(d)[dB]. \tag{6.6}$$

Here X_σ accounts for the shadowing loss due to obstructions. The shadowing component X_σ is modelled as a log-normal random variable. X_σ is Gaussian with mean zero and a variance σ^2 depending on the environment.

The log-normal distribution has a Probability Density Function (PDF) given as

$$g(x) = \frac{1}{\sqrt{2\pi}\sigma x} \exp\left(\frac{-\ln^2 x}{2\sigma^2}\right). \tag{6.7}$$

The corresponding Cumulative Distribution Function (CDF) is given by the equation

$$G(r) = \int_{-\infty}^{r} \frac{1}{\sqrt{2\pi}\sigma x} \exp\left(\frac{-\ln^2 x}{2\sigma^2}\right) dx. \tag{6.8}$$

The PDF and CDF can be graphically represented as shown in Figure 6.2 below.

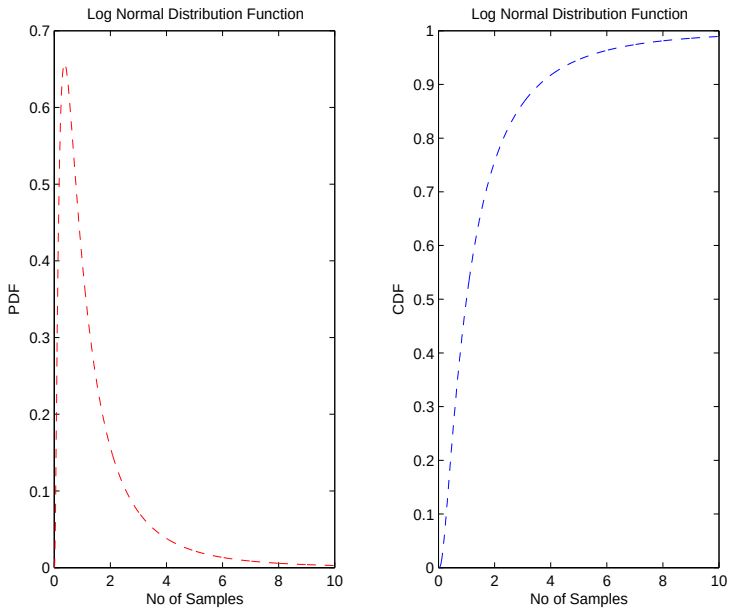

Figure 6.2: PDF and CDF of a log-normal distribution

6.3 Small Scale Fading

Small scale fading simply describes the rapid fluctuations in the amplitude, phases or delays of the multipath signal over shorter distances and time intervals, thus ignoring the large scale path losses. The multipath waves arrive at the receiver at different times giving rise to fading of the transmitted signal. The received signal envelope of the flat fading signal or a multipath signal can be best described by a Rayleigh distribution. The Rayleigh distribution has a PDF given by

$$p(r) = \frac{r}{\sigma^2} \exp\left(\frac{-r^2}{2\sigma^2}\right). \tag{6.9}$$

and the corresponding CDF is given as

$$P(R) = Pr(r \leq R) = \int_0^R p(r)dr = 1 - \exp\left(\frac{-R^2}{2\sigma^2}\right). \tag{6.10}$$

6.4 Channel Noise

The channel noise can be classified as being white or colored noise. The white noise is the result of un-coordinated interference from multiple sources in the surroundings. It is

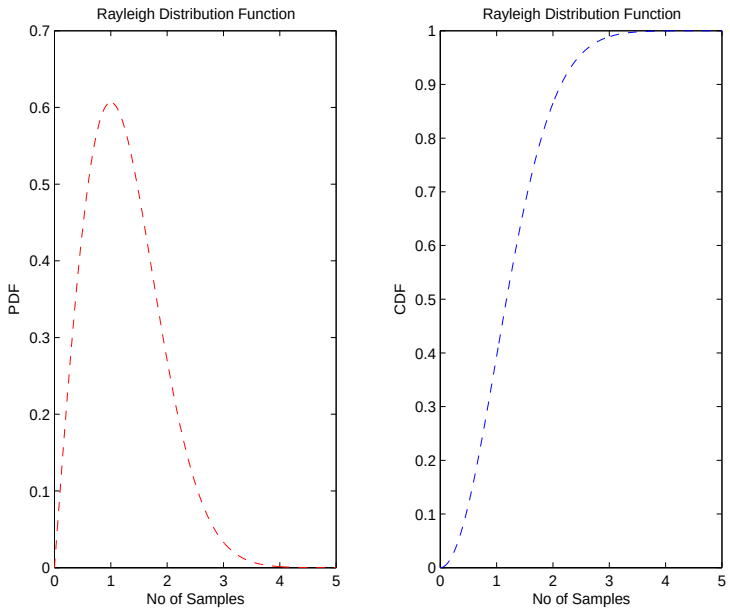

Figure 6.3: PDF and CDF of a Rayleigh distribution

generally modelled as a Gaussian random process with statistically uncorrelated successive samples. White noise is distributed evenly over the entire frequency band without any specific behavior over time and frequency. The white noise is commonly called as Additive White Gaussian Noise (AWGN) and is determined by the product of Boltzman constant k and the ambient temperature T.

$$N_0(dB) = 10\log_{10}(k\,T). \tag{6.11}$$

With $k = 1.38X10^{-23}$ and $T = 293$ K, we have $N_0(dB) = -203.93$ dB

Thus, the total noise in the system is given by the sum of the BT interfering signal (colored noise) and the AWGN channel noise.

6.5 Conclusions

This channel model will be used for the throughput analysis and optimization in Chapters 7, 8 and 9 to follow. Specifically, we aim to find an optimum packet size for each data rate of the 802.11b WLAN, in the presence and the absence of Bluetooth interference.

Chapter 7

Throughput Analysis of 802.11b WLAN

7.1 Introduction

The throughput measures the quality of a wireless link and is defined as the average number of information bits received without error per second. Naturally this quantity is desired to be as high as possible. The various factors affecting the throughput of a wireless systems are the packet size, the transmission rate, overheads of a packet, the received signal power, the noise power spectral density, the modulation schemes and the channel conditions. These variables can be used to calculate the important quantities such as the signal-to-noise ratio, the bit error rate P_e and the packet success rate. In this chapter, we present a throughput analysis using analytical expressions for each of the modulation schemes. The main objective of this analysis is to determine the optimum packet sizes for each of the data rates defined by the IEEE 802.11b. This analysis is based on the work by Dr. D. Goodman, M. Fainberg [1] and Shellhammer [15].

7.2 Packet Success Rate

The packet success rate is determined from the packet error rate of the system, which in turn is calculated based on the bit error rates of the system. For an indoor office or home

environment, we assume the bit error rate (P_e) to be independent from bit to bit. This assumption holds good for the indoor environment, where multiple reflections from the walls and ceilings lead to multiple copies of the same signal arriving at the receiver.

Let $\prod_{i=0}^{M}(1-P_{e,i})$ be the probability of correct reception of M bits. Then, the probability of correct reception of M bits with independent P_e is given as $(1-P_e)^M$. Thus the packet success rate is given as

$$\text{Packet Success Rate} = (1 - Pe)^M \tag{7.1}$$

and the packet error rate (PER) is given as

$$\text{PER} = 1 - \text{Packet Success Rate} = 1 - (1 - P_e)^M \tag{7.2}$$

where M is the number of bits in each packet.

7.3 Packet Transmit Time

A data packet in 802.11b is composed of an overhead portion containing the preamble and header and the data portion. The transmit time of an 802.11b packet can be calculated using the Equation (7.3) as follows

$$t_T = \text{DIFS} + \text{Overhead} + \frac{\text{Data(bits)}}{\text{Rate(bits/sec)}} + \text{SIFS} + \text{ACK}. \tag{7.3}$$

The inter-frame spaces DIFS and SIFS are considered to ensure correct reception of the packet. The 802.11b MAC defines the timing intervals for the various inter-frame spaces. Thus we have,

$$\text{DIFS} = 50\mu s, \qquad \text{SIFS} = 10\mu s, \qquad \text{ACK} = 112\mu s$$

$$\text{Overhead} = \text{Preamble } (144\mu s) + \text{Header } (48\mu s) = 192\mu s.$$

The average time for a successful reception can be calculated as

$$T_w = t_T + (1-p)\sum_{i=1}^{\infty} i\, p^i\, t_T \tag{7.4}$$

The equation states that the i^{th} retry packet must have been delivered i times with the probability of correct reception on the i^{th} try being $(1-p)$. The equation can be further simplified using formulas as

$$\begin{aligned}(1-p)\sum_{i=1}^{\infty} i\,p^i\,t_T &= t_T\,p\,(1-p)\sum_{i=1}^{\infty} i\,p^{i-1} = t_T\,p\,(1-p)\frac{d}{dp}\left[\sum_{i=1}^{\infty}\left(\int i\,p^{i-1}\right)\right] \\ &= t_T\,p\,(1-p)\frac{d}{dp}\left[\sum_{i=1}^{\infty} p^i\right] = t_T\,p\,(1-p)\frac{d}{dp}\left[\frac{p}{1-p}\right] \\ &= t_T\,p\,(1-p)\frac{1}{(1-p)^2} = \frac{t_T\,p}{(1-p)}.\end{aligned} \tag{7.5}$$

Thus, the average time T_w can be calculated as

$$T_w = t_T + (1-p)\sum_{i=1}^{\infty} i\,p^i\,t_T = t_T + \frac{t_T\,p}{(1-p)} = \frac{t_T}{(1-p)}. \tag{7.6}$$

The throughput is the actual data bits sent per packet transmission time with a certain probability of success called the packet success rate. Thus, we have

$$\text{Throughput} = \frac{\text{Data}}{T_w} = \frac{\text{Data}}{t_T}(1-p) = \frac{\text{Data}}{t_T}\ (\text{Packet Sucess Rate}). \tag{7.7}$$

With a data size of 1000 bytes, the packet times for the various data rates are as shown in the Table 7.1below

Rate	1 Mbps	2 Mbps	5.5 Mbps	11 Mbps
t_T	8.4 msec	4.2 msec	1.6 msec	1.1 msec

Table 7.1: Packet Transmit Timings

The throughput of the 802.11b in the fading multipath channel can be shown in the Figure 7.1. The analytical expressions for CCK 5.5 and 11 Mbps have not been derived. CCK is a variation of M-ary Bi-Orthogonal Keying with complex codewords. Hence, for this analysis, the analytical expressions for M-ary Bi-Orthogonal Keying [24, 4, 26, 1] have been used. However, the throughput simulator implemented in Chapter 10 simulates the CCK modulation as specified in the IEEE 802.11b standard [25].

As seen from Figure 7.1, the CCK 11 Mbps scheme performs best for the first 30-35 meters. For the next 5-10 meters, the 5.5 Mbps CCK gives the best available throughput.

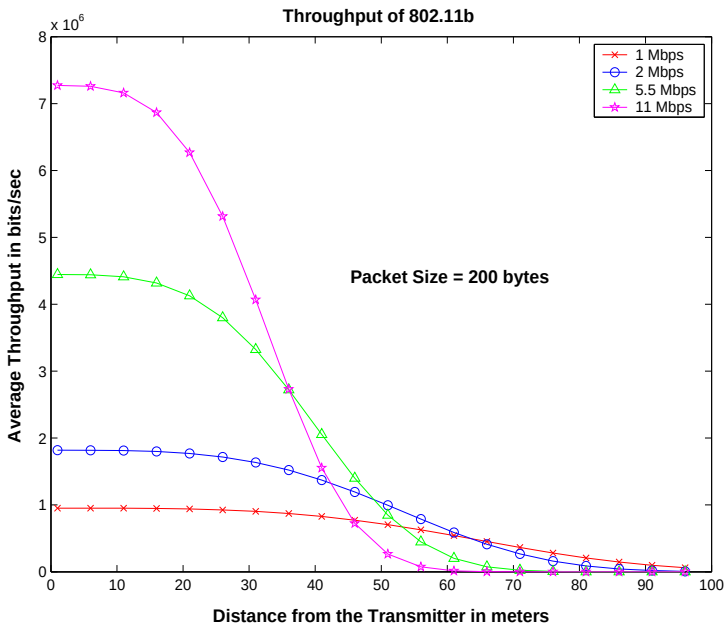

Figure 7.1: Throughput of 802.11b in a Fading Channel

Similarly the lower data rate modulation schemes namely, the 2 Mbps DQPSK performs efficiently for the next 20 meters. The 1 Mbps DPSK gives the best throughput from 65 meters to 100 meters.

The transmit power of the IEEE 802.11b here is 100 mW or 20 dBm. The packet length is chosen to be 200 bytes. The next section discusses the use of fragmentation as proposed by the IEEE 802.11 standard for optimizing the throughput at each of the data rates.

7.4 Need for Throughput Optimization

In order to optimize the throughput, we need to optimize the throughput of each of the data rates. The PER of the system depends on the packet sizes and increases with the increasing packet sizes. An increase in the packet sizes leads to an increase in throughput to a certain limit. Hence, controlling the packet sizes at each of the data rates can optimize the throughput of the system. The main idea is to find a packet size which gives the best throughput within the operating range of the system. This is possible due to fragmentation in the IEEE 802.11b standard. The fragment sizes can vary from 100 bytes to 2350 bytes.

As seen from the Figure 7.1, the 11 Mbps scheme gives the best throughput in the first 30 meters, hence we analyze the throughput within the first 30 meters. Similarly we observe the throughput of the 5.5 Mbps scheme in the range 30-40 meters, the 2 Mbps scheme in the range 40-60 meters and the 1 Mbps DPSK in the range 60-90 meters.

7.5 Throughput Optimization

To optimize the throughput for the first 30 meters, we fix the distance from the 802.11b transmitter and observe the throughput with varying packet sizes from 100 bytes to 2350 bytes. The throughput curves for 10, 20 and 30 meters are plotted for the 11 Mbps CCK scheme as shown in Figure 7.2.

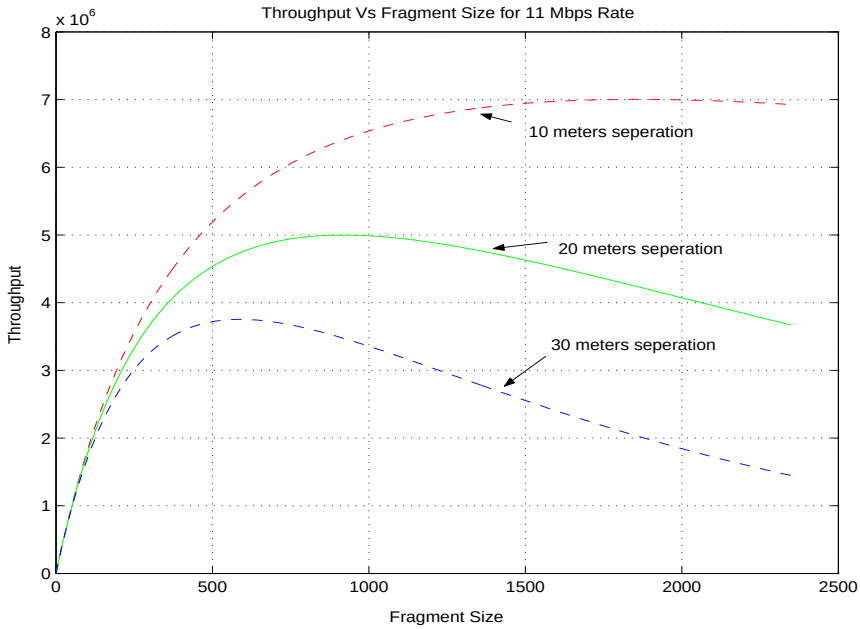

Figure 7.2: Packet Optimization for 11 Mbps Rate

As seen from Figure 7.2, the best packet sizes for the 11 Mbps rate is about 1750 bytes giving throughput in excess of 7 Mbps. For 20 meters distance, the throughput reaches rates of about 5 Mbps with packet sizes of approximately 800 bytes. To optimize the throughput for the 11 Mbps rate, we select a packet size of 1750 bytes for optimizing the throughput within the first 30 meters for the 11 Mbps rate.

The throughput for the 5.5 Mbps is best observed between 30 to 40 meters as observed from Figure 7.1. As seen from Figure 7.3, the throughput reaches about 2.8 Mbps with packet size of 600 bytes for 30 meters separation from the transmitter and 2.6 Mbps with 35 meters separation with the same packet size. However, the 30 meters intersects partly with the range of the 11 Mbps CCK data rate; hence we choose 35 meters as the optimum region of operation for the 5.5 Mbps CCK rate.

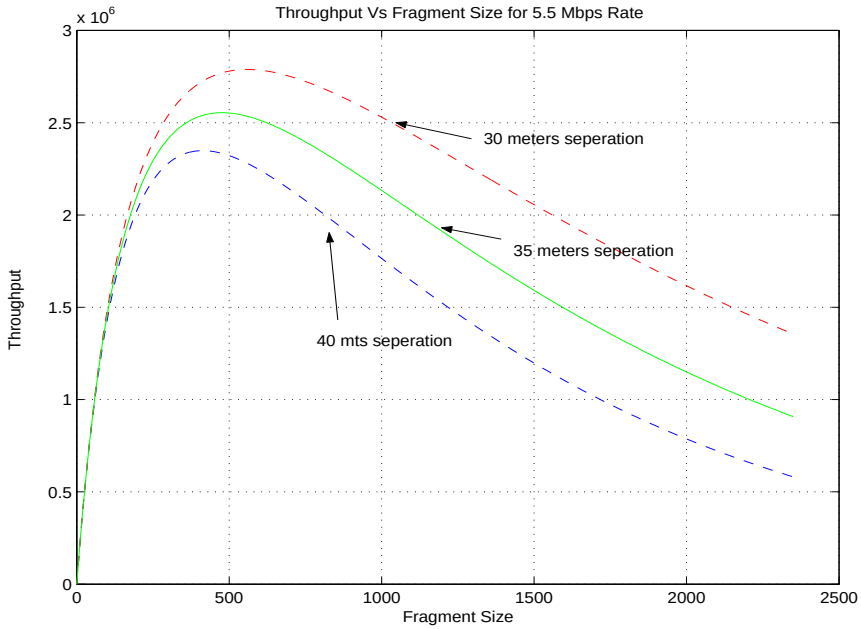

Figure 7.3: Packet Optimization for 5.5 Mbps Rate

The best possible packet size for the 5.5 Mbps rate is 600 bytes giving a throughput of about 2.6 Mbps at 35 meters. Hence, we select this packet size to optimize the throughput for the 5.5 Mbps data rate.

The 2 Mbps data rate performs best for distances between 40 to 60 meters as seen from Figure 7.1, hence we analyze the throughput for the 2 Mbps rate for distances ranging from 40 meters to 60 meters as shown in Figure 7.4. The 2 Mbps DQPSK scheme gives throughput of about 1.6 Mbps at distance of 40 meters and about 1.4 Mbps at distance of 50 meters. As before the 40 meters range coincides with the CCK 5.5 Mbps range of operation, hence we select the 50 meters distance for giving the best throughput with the 2 Mbps rate. A packet size of about 400 bytes is selected to optimize the throughput for the 2 Mbps data rate.

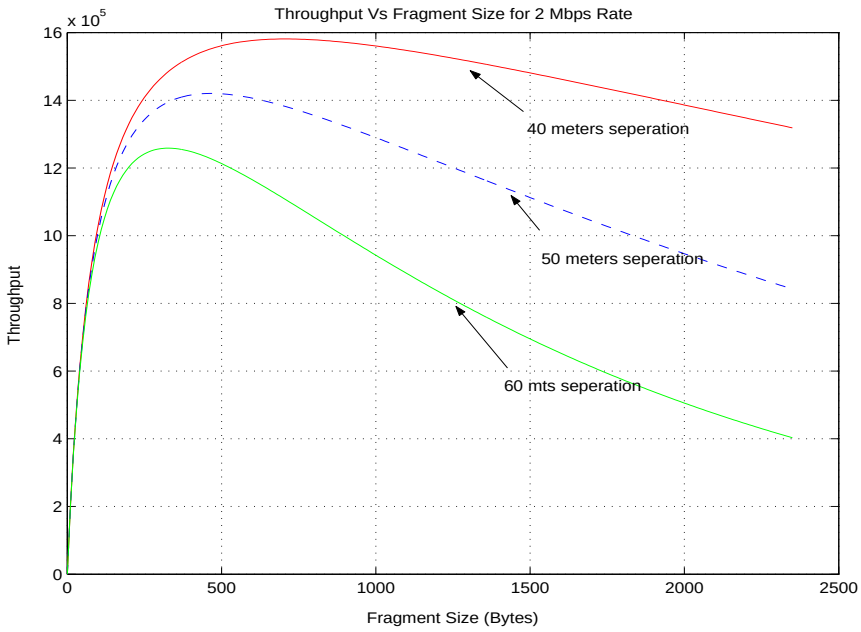

Figure 7.4: Packet Optimization for 2 Mbps Rate

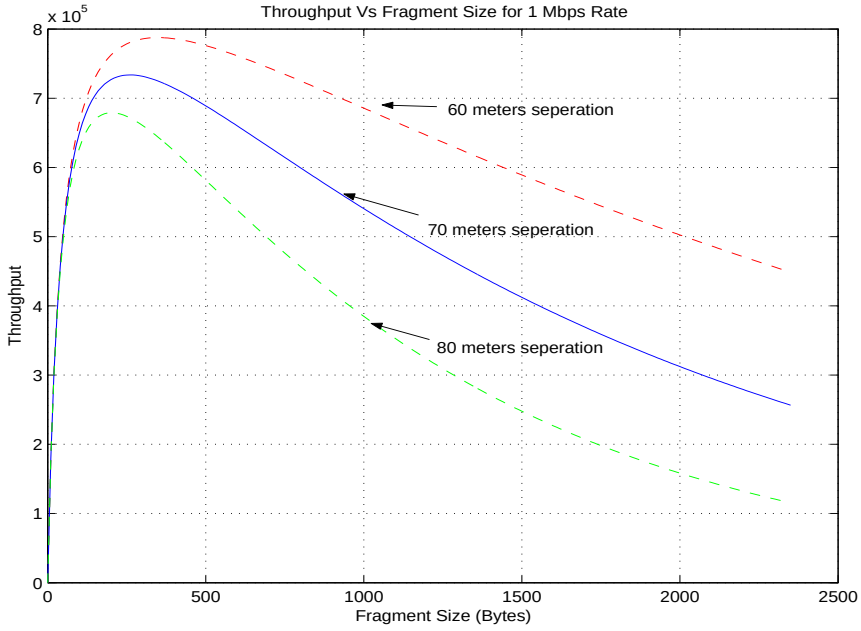

Figure 7.5: Packet Optimization for 1 Mbps Rate

The 1 Mbps data rate operates best from distances 60 meters onwards. The throughput is analyzed for distances ranging from 60 meters to 80 meters. As seen from Figure 7.5, we obtain a throughput of around 800 Kbps at 60 meters. The throughput reaches a maximum

of 750 Kbps for 70 meters distance. Due to interference with the 2 Mbps region, the best distance for operation with the 1 Mbps data rate is selected to be from 70 meters onwards. The optimum packet size for this range is about 300 bytes as can be seen from Figure 7.5.

Rate	1 Mbps	2 Mbps	5.5 Mbps	11 Mbps
Optimum Packet Size	300 bytes	400 bytes	600 bytes	1750 bytes

Table 7.2: Optimum selected packet sizes

Using these selected packet sizes, we can plot the throughput for all the four data rates against the distances from the receiver and compare the graph thus generated against the Figure 7.1 with fixed packet sizes of 200 bytes.

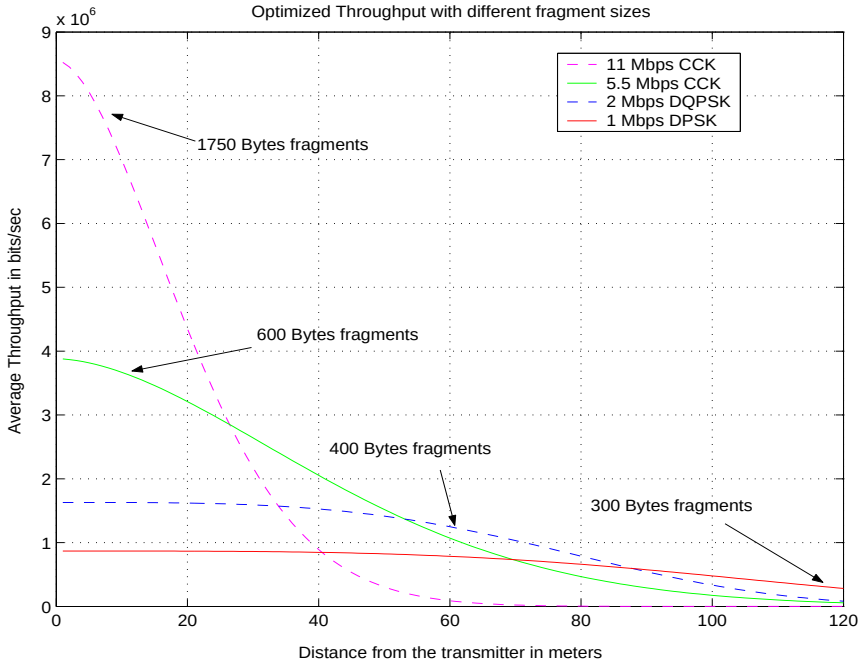

Figure 7.6: Optimized throughput

As seen from the figure, the optimized throughput reaches rates of almost 8.5 Mbps for the first 2-3 meters as against the throughput of around 7 Mbps with fixed size packets. The optimized throughput degrades from 8.5 Mbps to 7 Mbps for the first 10 meters. For distances ranging from 20 meters to 40 meters, with CCK 5.5 Mbps, the throughput degrades from 4 Mbps to 2 Mbps as against 4 Mbps to 1.5 Mbps in Figure 7.1. From distance 40

meters onwards, the throughput degrades from 2 Mbps to only 1.5 Mbps compared to Figure 7.1 where the throughput drops from 1.5 Mbps to 0.5 Mbps. The operating range of the system also increases slightly to about 120 meters with optimized packet sizes.

Thus, we can tabulate our results against the throughput obtained in Figure 7.1 as shown.

Rate	11 Mbps	5.5 Mbps	2 Mbps	1 Mbps
Range	1-30 meters	30-40 meters	40-60 meters	60-100 meters
Throughput in Mbps	7.2-2.5	2.5-1.7	1.7-0.7	0.7-0.001

Table 7.3: Throughput with fixed packet sizes

Rate	11 Mbps	5.5 Mbps	2 Mbps	1 Mbps
Range	1-30 meters	30-50 meters	50-90 meters	90-120 meters
Throughput in Mbps	8.5-3	3-1.5	1.5-0.6	0.6-0.2

Table 7.4: Throughput with different packet sizes

7.6 Conclusions

The performance improvement in terms of the distance of operation as well as the increase in throughput can be seen from the data in the tables shown above and the Figure 7.6. However, as we already know, the increase in the size of the packets also increases the packet error rate. Hence a tradeoff between the allowed packet error rate and the throughput is desired according to the various channel conditions. This idea of throughput optimization motivates the future work of a Link Adaption Strategy to balance the throughput for small range of distances with an acceptable packet error rate for the system for the given channel conditions. In the next chapter define the network topology used for the throughput analysis in the presence of Bluetooth interferer.

Chapter 8

Network Topology

8.1 Introduction

The 802.11b Wireless LAN and the Bluetooth Personal Area Network (PAN) will co-exist in different network configurations. The 802.11b system performance is affected depending upon the network configuration in which it exists. We define two distinct network topologies, namely the Office Network and Home Configuration for the co-existence of 802.11b WLAN and Bluetooth PAN.

8.2 Home Configuration

This scenario generally involves a wireless access point (AP), i.e., the 802.11b Transmitter and one 802.11b receiving station (STA) which might be a desktop or a laptop. Figure below shows a typical household network with one AP and one STA.

This network has a single Bluetooth interferer located within close proximity (1-5 meters) of the 802.11b receiving station. The Bluetooth signal also suffers from a path loss as it interferers with the 802.11b receiver. However the Bluetooth transmitter transmits at lower power (1mW or 0dBm) than the 802.11b transmitter (100mW or 20dBm). The 802.11b LAN suffers from loss in network throughput during the transmission from the access point (AP) to the receiving station (STA) as shown in the figure 8.1. An alternative configuration also exists where the STA transmits data to the AP with the Bluetooth interferer in the

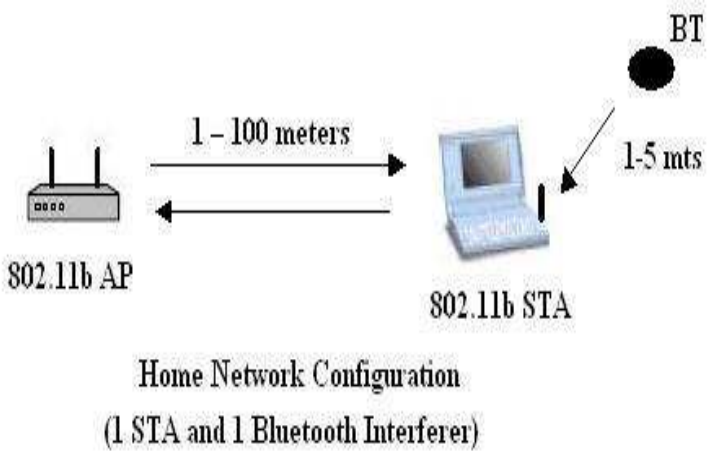

Figure 8.1: Home network configuration

vicinity of the AP. The loss in performance in both the cases is considered to be the same. We evaluate the loss in performance due to the case described in Figure 8.1.

8.3 Small Office network

The small office network consists of one or more access points (APs) and receiving stations (STAs) in a network as shown in Figure 8.2 below.

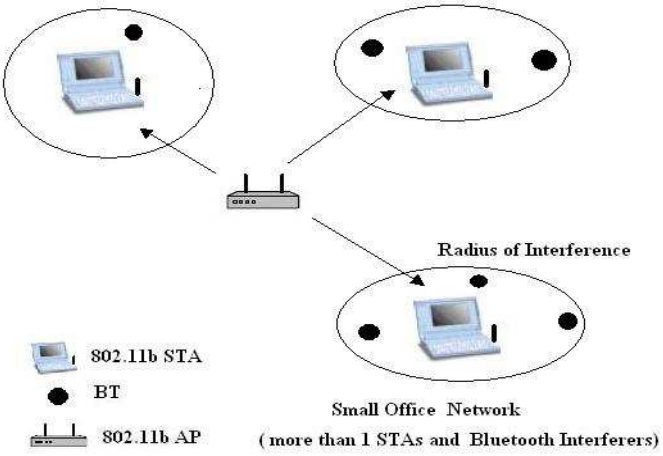

Figure 8.2: Small Office network

The Bluetooth interferers are located in a radial fashion around the 802.11b receiving station. The loss in the network throughput is more in this scenario due to the presence of more Bluetooth interferers. All the Bluetooth interferers are assumed to be located in close proximity of the 802.11b receiving station. The corresponding sections examine the throughput of the 802.11b receiver with Bluetooth interference for both the network configurations discussed above.

8.4 Conclusions

With the network topologies defined above, we will replicate the analysis of Chapter 7, with the existence of Bluetooth interferers. As before, we will also try to optimize the throughput by selecting different optimum packet sizes for each data rate.

Chapter 9

Throughput Analysis of 802.11b WLAN with BT interference

9.1 Introduction

The Bluetooth system is a fast frequency hopping system. As a result, it combats the possible interference from other devices by fast hopping to another frequency slot. The Bluetooth data packets are much smaller than the 802.1b, hence it takes smaller amount of time for retransmission as compared to the time needed for the retransmission of the 802.11b packets. As a result, the 802.11b suffers more from the Bluetooth interference than the 802.11b affecting Bluetooth.

9.2 802.11b Interference with Bluetooth

The Bluetooth transmitter transmits with a low power of 1mW or 0dBm in contrast to the 802.11b which transmits with a power of 100 mW or 20 dBm. We assume that both the devices suffer from the same path loss with their respective transmit powers. The Signal-to-Interference and Noise Ratio (SINR) is defined as

$$\text{SINR} = \frac{\text{Signal power from the 802.11b}}{(\text{Noise} + \text{Signal power from BT interferer})\ \text{Chip Rate}}. \tag{9.1}$$

Now, considering the home network configuration as described earlier, the path loss for the Bluetooth interferer at a distance of 1-10 meters from the 802.11b receiver can be modelled in a manner similar to the path loss for the 802.11b receiver.

For the evaluation of throughput the probability of packet error, (PER) of the system is of greater interest. The probability of collision between the 802.11b and the Bluetooth at the physical layer is represented by P_e and at the MAC layer is represented by P_o.

The BT and 802.11b packets have to overlap in frequency and time to have a collision between them. Bit errors will occur when the SINR is sufficiently low. Figure 9.1 below helps us to find out the PER for an 802.11b system with a Bluetooth interferer.

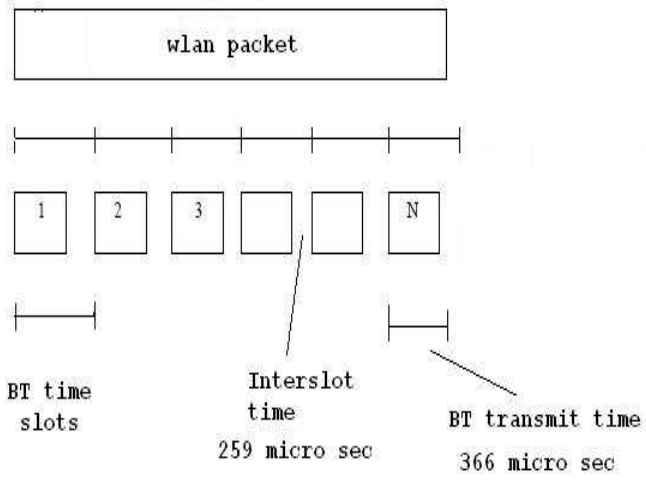

Figure 9.1: Time collision of WLAN and Bluetooth packets

The Bluetooth system transmits every $625\mu s$. However out of the $625\mu s$, the actual data transmission takes place for $366\mu s$. The remaining $259\mu s$ is considered to be the idle time, or the inter-slot time. Thus, we consider the slot error rate of the system first and then derive the packet error rate from it [1, 15].

The Slot Error Rate is given as

$$\text{SER} = \text{P}\{\text{Bad Slot}\} = 1 - \text{P}\{\text{Good Slot}\}$$

$$\text{P}\{\text{Good Slot}\} = \text{P}\{\text{Good/Collision}\}\ \text{Po} + \text{P}\{\text{Good/NoCollision}\}\ \text{(1-Po)}$$

$$\text{P\{Good/NoCollision\}} = (\text{1-Pe\{No BT Int }\})^{bits\ in\ 625\mu s}$$

$$\text{P\{Good/Coll\}} = (\text{1-Pe\{BT Int\}})^{bits\ in\ 366\mu s} \quad (\text{1-Pe\{No BT Int\}})^{bits\ in\ 259\mu s}$$

The probability of the WLAN packet to be good for the $366\mu s$ is defined by the first term where as the second term defines the probability of a good WLAN packet for the remaining $259\mu s$. In the frequency domain, the probability of overlap is defined by $P_o = (22/79)$. Here the value 22/79, is the probability of interference between the BT and 802.11b in the frequency domain.

$$\text{P\{Good 802.11b packet\}} = \text{P\{Good Slot\}}^N$$

$$\text{PER} = 1 - \text{P\{Good 802.11b packet\}} \tag{9.2}$$

Let N be the number of BT data slots that overlap the 802.11b packet. For each data rate, N is calculated by the ratio of the 802.11b packet transmission time (t_T) to the Bluetooth transmission time ($625\mu s$). For an office environment, we can set the number of Bluetooth piconets to n and, get the derivation for PER as

$$\text{PER}_{\text{multiple piconets}} = 1 - (1 - \text{PER})^n \tag{9.3}$$

The throughput of the 802.11b is plotted in Figure 9.2 against the received signal strength of the 802.11b signal for all the four data rates. The throughput of the 802.11b with the 2 BT interferers is as shown in Figure 9.3. The presence of the additional Bluetooth interferer completely degrades the 1 and the 2 Mbps data rate throughput. The higher data rates also experience significant degradation in the throughput.

However, this analysis does not consider the effects on DSSS spreading to reduce the bluetooth interference. The use of DSSS would increase the resistance to BT interference and the range of operation of the 1 and 2 Mbps data rates. In the next chapter, we present a complete simulation with the effects of DSSS spreading.

9.3 Throughput Optimization

This section optimizes the throughput for the 802.11b LAN in the presence of a BT interfering piconet. As we know, an increase in the packet sizes leads to an increase in

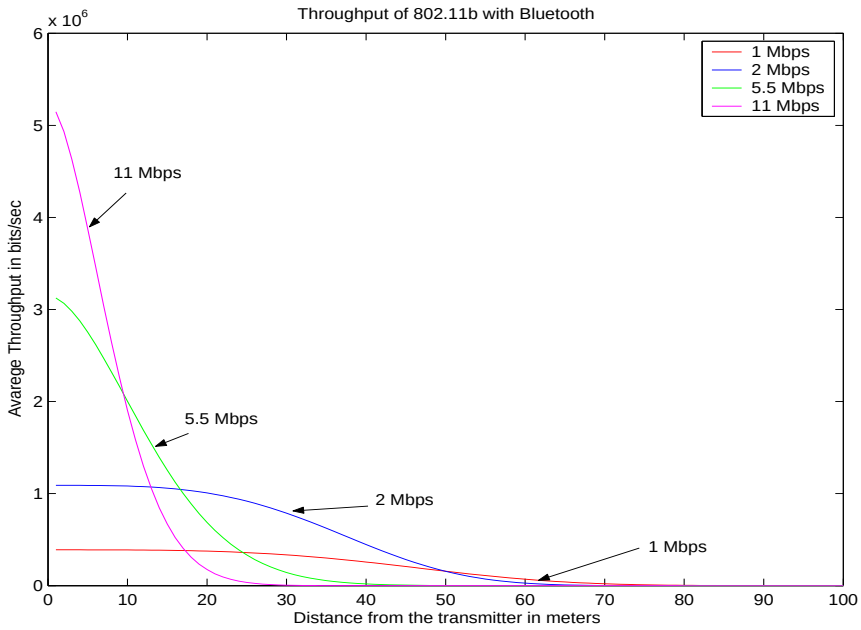

Figure 9.2: Throughput of 802.11b with Bluetooth interferer

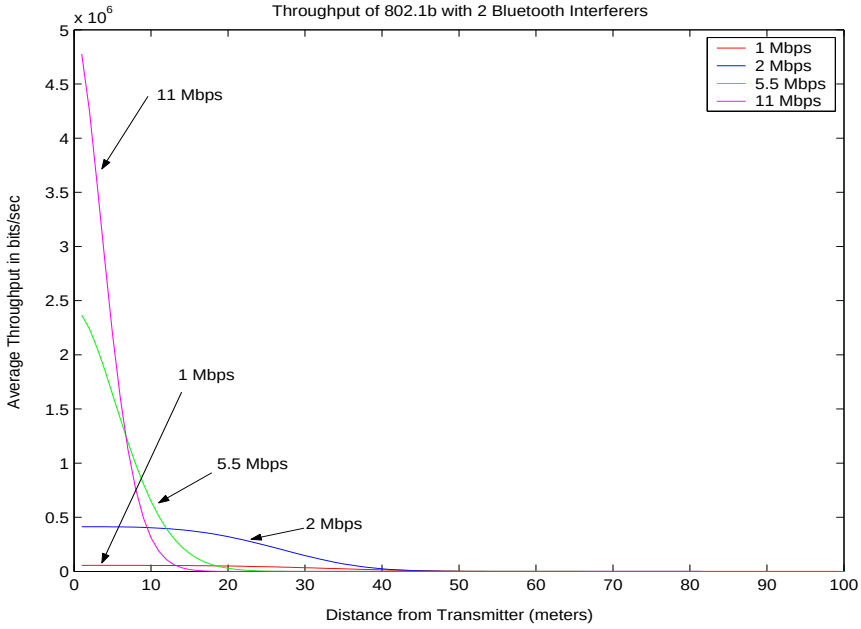

Figure 9.3: Throughput of 802.11b with 2 Interfering piconets

throughput to a certain limit. Hence, controlling the packet sizes at each of the data rates can optimize the throughput of the system. Thus, we aim to find a packet size which gives the best throughput within the operating range of the system. Due to fragmentation in the

IEEE 802.11b standard the fragment sizes can vary from 100 bytes to 2350 bytes.

From Figure 9.2, the 11 Mbps scheme gives the best throughput in the first 15 meters; hence we analyze the throughput within the first 15 meters. Similarly, the throughput of the 5.5 Mbps scheme is in the range 10-20 meters, the 2 Mbps scheme in the range 20-40 meters and the 1 Mbps DPSK in the range 40-70 meters.

To optimize the throughput for the first 10 meters, we fix the distance from the 802.11b transmitter and observe the throughput with varying packet sizes from 100 bytes to 2350 bytes. The throughput curves for 5, 10 and 15 meters are plotted for the 11 Mbps CCK scheme as shown in Figure 9.4 below.

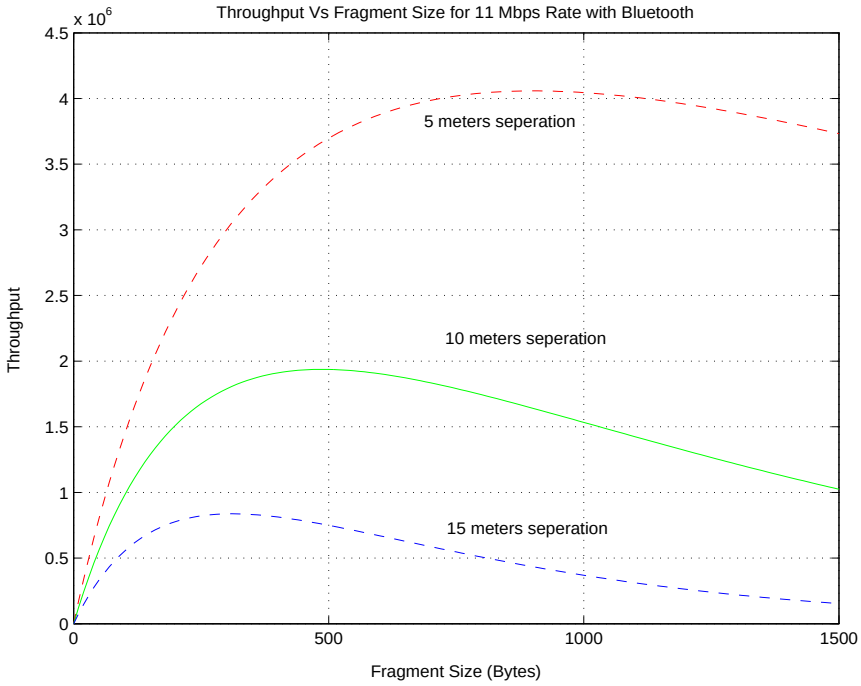

Figure 9.4: Packet Optimization for 11 Mbps Rate

As seen from the figure, the best packet sizes for the 11 Mbps rate is about 800 bytes, giving throughput in excess of 4 Mbps. For 10 meters distance, the throughput reaches rates of about 2 Mbps with packet sizes of approximately 500 bytes. Thus, we select a packet size of 800 bytes for optimizing the throughput within the first 15 meters for the 11 Mbps rate.

The throughput for the 5.5 Mbps is best observed between 10 to 20 meters as observed from the Figure 9.2. As seen from Figure 9.5, the throughput reaches about 2.2 Mbps with

packet size of 400-450 bytes for 10 meters separation from the transmitter and 1.4 Mbps with 15 meters separation with the same packet size.

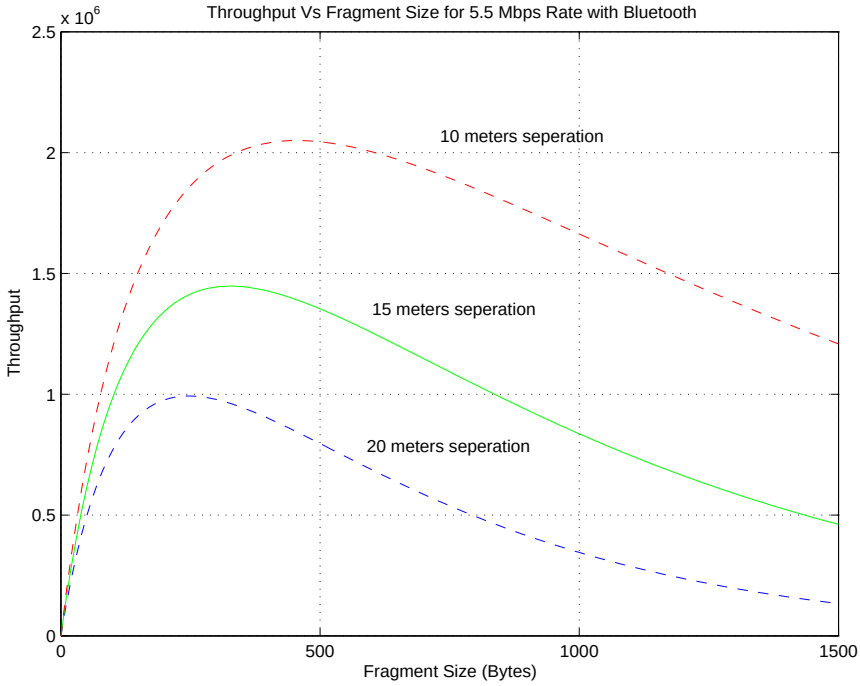

Figure 9.5: Packet Optimization for 5.5 Mbps Rate

The best possible packet size for the 5.5 Mbps rate is 450 bytes giving a throughput of about 2.2 Mbps at 10 meters. Hence, we select this packet size to optimize the throughput for the 5.5 Mbps data rate. Similarly we try to optimize the throughput for the 1 and the 2 Mbps rates operating in the ranges 40-70 meters and 20-40 meters in Figures 9.6 and 9.7 respectively.

Rate	1 Mbps	2 Mbps	5.5 Mbps	11 Mbps
Optimum Packet Size	150 bytes	300 bytes	450 bytes	800 bytes

Table 9.1: Optimum Packet Sizes

With these packet sizes, we can plot the throughput for all the four data rates against the distances from the receiver in Figure 9.8 and compare the graph thus generated against Figure 9.2 with fixed packet sizes.

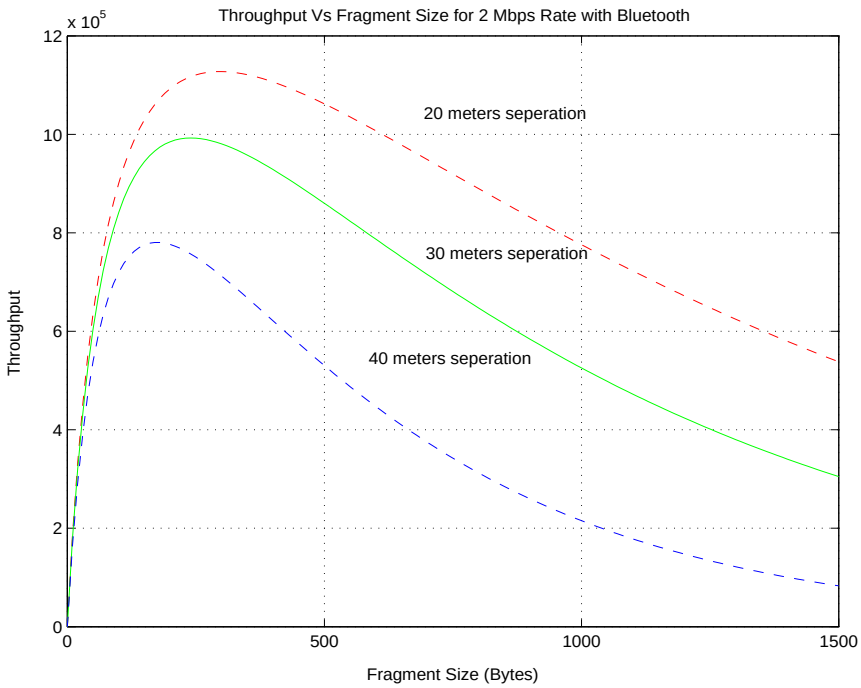

Figure 9.6: Packet Optimization for 2 Mbps Rate

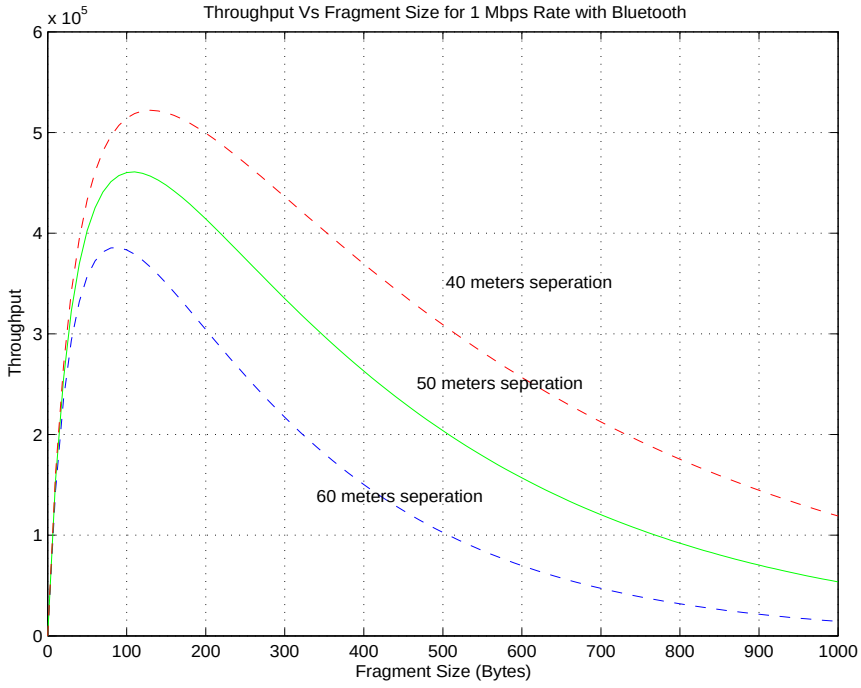

Figure 9.7: Packet Optimization for 1 Mbps Rate

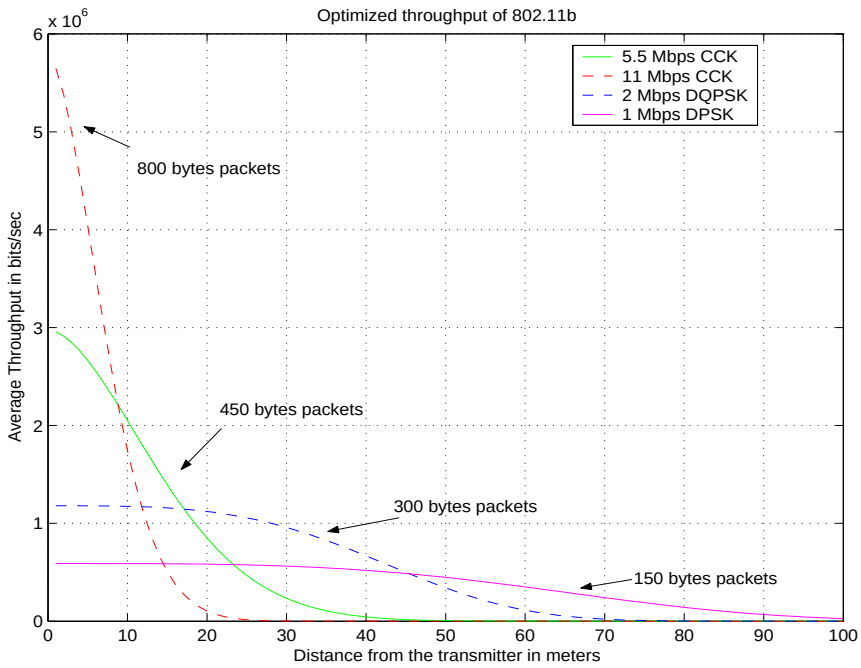

Figure 9.8: Optimized throughput with Bluetooth interference

9.4 Conclusions

Comparing Figures 9.2 and 9.8 we find that there is a little improvement in the throughput. Some improvements can be specifically noted as follows

The fixed packet size throughput reaches a maximum of 5.1 Mbps as opposed to the 5.6 Mbps throughput with variable optimized packet sizes. We observe a small increase in throughput for each distance. Overall, the range of the system increases to about 100 meters as compared with the 70-80 meters range earlier.

This analysis serves as a starting point for the simulations to follow. In the next chapter, we will use the optimized packet sizes to determine the actual effects of Bluetooth on the performance of 802.11b. The use of 11 chip DSSS increases the resistance of the 1 and 2 Mbps systems, compared to the 5.5 and 11 Mbps CCK with no spreading. Thus justifies the use of these lower data rates over larger distances. We try optimize the throughput for each data rate using a variety of different techniques namely, Maximal Ratio Combining (MRC) and Space Time Coding (STC). A final attempt to cancel the BT interference and noise is made using Interference Rejection Combining (IRC).

Chapter 10

The IEEE 802.11b Throughput Simulator

10.1 Introduction

In this chapter, we present results of throughput simulations for a variety of different receivers and discuss the performance improvements resulting from them. This baseband simulation does not implement the PHY Protocol Data Units frame (PPDU), which contains all the necessary information for synchronization and hence the problem of synchronization is not considered.

As discussed before, randomly generated data is modulated with the appropriate 802.11b WLAN modulation scheme and pulse shaped with a square-root-raised-cosine filter having a roll-off factor of 0.5. The signal thus generated is transmitted over the channel. The presence of Bluetooth interference and the channel gains corrupt the signal as it arrives at the receiver. At the receiver, the signal is subjected to low-pass filtering and pulse shaping by the square-root-raised-cosine filter. The filtered signal is then decoded and demodulated with the appropriate demodulators. Our simulator then looks at each packet to see if an error has occurred. We then compare the total transmitted packets to the packets received with errors and compute the packet error rate as

$$\text{Packet Error Rate(PER)} = \frac{\text{Packets in Error}}{\text{Transmitted Packets}} \tag{10.1}$$

We present results for a slow flat fading channel with a single antenna receiver, for 1 Mbps DPSK scheme with the upper and lower bounds for the best and the worst case scenarios. The lower data rates, namely 1 and 2 Mbps use 11-chip DSSS spreading as opposed to no DSSS spreading used by CCK.

The use of multiple receive antennas increases the throughput performance and range of the devices to some extent. In particular, we observe the improvement in throughput using Maximal Ratio Combining (MRC) technique with 1 transmit and 2 receive antennas [18].

Some commercially available 802.11b routers use 2 transmit antennas and BPSK, QPSK modulation schemes for data rates of 1, 2 Mbps. Hence, the performance improvement of the 1 Mbps BPSK modulated 802.11b signal using multiple transmit antennas (space time codes) over a single antenna transmitter-receiver is demonstrated.

The 802.11b system is not considered complete without the use of error detection and correction. The error detection and correction have not been implemented in this report. However we present simulation results showing an improvement in throughput assuming error detection and correction for the 1 Mbps modulation scheme. Finally, we aim to suppress the interference caused by the Bluetooth interferer, by using an Interference Cancellation Technique [18].

10.2 Signal Model

In this section, we discuss the signal model used in the simulations. In the earlier chapters, we considered the relative bit energies of the Bluetooth and the 802.11b signals with a slow flat fading channel. In this section, we consider a more realistic implementation of the channel model with the presence of small scale and large scale fading. The actual transmit powers of the WLAN and the BT schemes are taken into consideration.

For this signal model, the received signal r can then be expressed in discrete time as

$$\boldsymbol{r} = P_{wlan}\, h_1 \boldsymbol{s_{wlan}} + P_{bt}\, h_2 \boldsymbol{s_{bt}} + \boldsymbol{w} \tag{10.2}$$

with $P_{wlan} = \frac{\sqrt{E_{b\,wlan}}}{d^n}$ and $P_{bt} = \frac{\sqrt{E_{bbt}}}{{d_{bt}}^n}$ being the large scale fading coefficients for the

WLAN and the BT systems respectively and $w \sim (0, \frac{N_0}{2})$. The noise power spectral density N_0 is given as, $N_0 = kT$ where k is the Boltzman's constant and T being the ambient room temperature.

Here $E_{bwlan} = 100mW \times t_{wlan}$, and $E_{bbt} = 1mW \times t_{bt}$ are the received bit energies of the WLAN and BT signals, with symbol durations given by t_{wlan} and t_{bt} respectively. The channel coefficients h_1 and h_2 account for the amplitude variations due to small scale fading. The path loss increases with increasing distance between the transmitter and the receiver, and accounts for the large scale fading. The distance between the WLAN transmitter and the receiver is given by d, and the distance of BT network from WLAN receiver is given by d_{bt}. The path loss coefficient n for the indoor environment is generally between 2 and 4.

The performance of the WLAN system improves as the distance between the interfering BT network and the WLAN receiver increases. We plot the throughput curves for distances of 2, 5 and 8 meters between the BT network and the WLAN receiver for a 1 Mbps DPSK system with DSSS spreading.

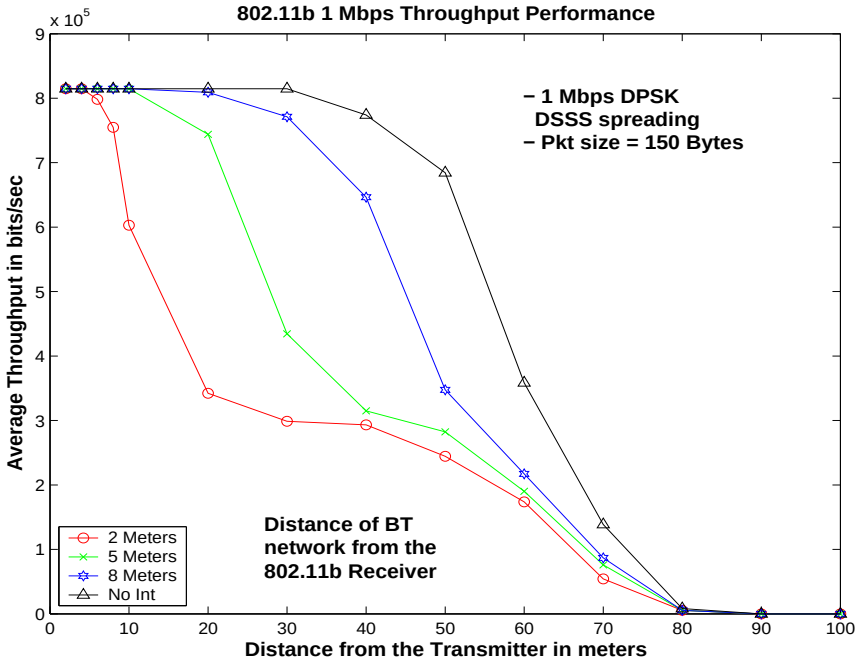

Figure 10.1: Throughput Performance for different Bluetooth network topologies

As seen from Figure 10.1, the WLAN performance improves with increasing distance

between the WLAN receiver and the BT network. For the remainder of the chapter, we fix the distance between the BT network and the WLAN receiver to 4 meters. We consider the channel model as discussed in (10.2), with a path loss exponent of 3.5.

10.3 Flat-fading Channel with Single Antenna Receiver

In this section, we present the upper and lower bounds for the best and worst case possibilities with Bluetooth interference. The best case occurs when the Bluetooth interferer always hops to a different frequency channel. In this case the 802.11b LAN is not affected by BT during its entire transmission period. Thus we have the system performance equivalent to the one without the presence of any BT interferer. Conversely, the worst case scenario occurs when the BT interferers always hops to a frequency in use by the 802.11b channel. This always results in collisions between the WLAN packet and the BT packet. The average throughput for an 802.11b system with BT interferer occurs with random collisions in time and frequency between the WLAN and BT packets. The collisions in frequency are modelled by an random variable in these simulations. Figure 10.2 below shows the upper and lower bounds and the average throughput for a 1 Mbps DPSK system with BT interference.

We present similar results for the 1 Mbps BPSK system. The BPSK system performs marginally better than the BPSK system on account of its better bit error rate (BER). Figure 10.3 below shows the upper and lower bounds and the average throughput for a 1 Mbps BPSK system with BT interference.

10.4 Throughput Improvement using Multiple Receive Antennas - Maximum Ratio Combining Scheme

In the Maximal Ratio Combining Scheme (MRC), the signals from all the branches are weighted according to their individual SNR and then added. The weighing and addition produces the output with an acceptable SNR value when none of the individual signal valued signals are acceptable.

For a system deploying 1 Transmit and 2 Receive antennas, the 2 received signals can be

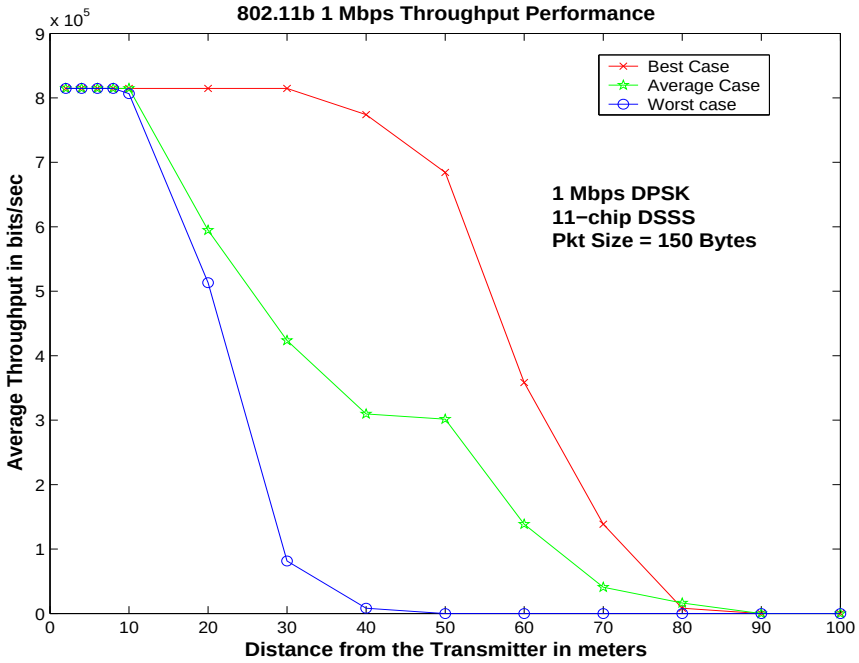

Figure 10.2: Upper and Lower bounds on the throughput of DPSK with Bluetooth Interference

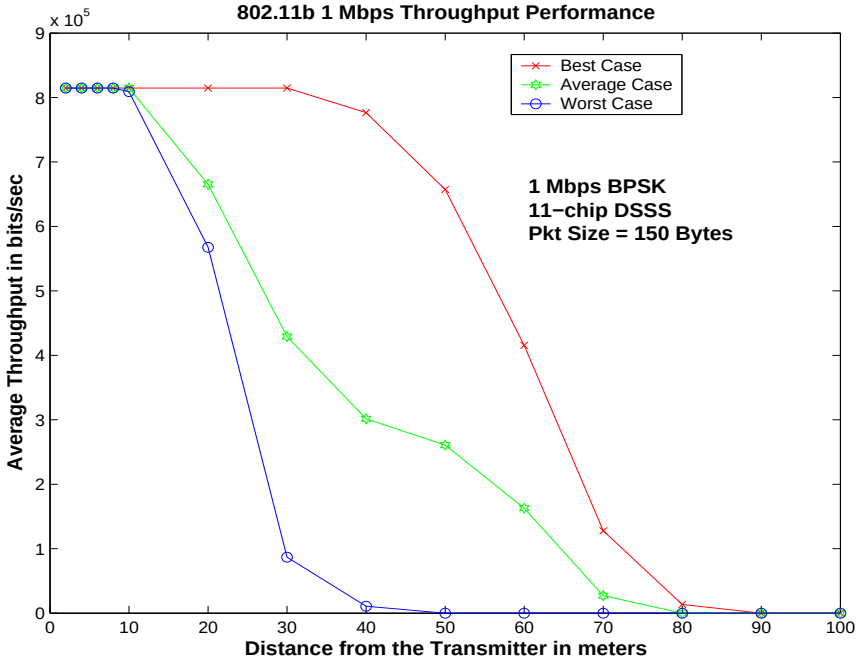

Figure 10.3: Upper and Lower bounds on the throughput of BPSK with Bluetooth Interference

modelled as

$$\boldsymbol{r_1} = h_{11}\boldsymbol{s_{wlan}} + h_{21}\boldsymbol{s_{bt}} + \boldsymbol{w_1} \tag{10.3}$$

and

$$\boldsymbol{r_2} = h_{12}\boldsymbol{s_{wlan}} + h_{22}\boldsymbol{s_{bt}} + \boldsymbol{w_2}. \tag{10.4}$$

Here we have dropped the large scale fading coefficients for simplicity. The channel coefficients $h_{11}, h_{12}, h_{21}, h_{22}$ are given by Equation (10.5) with α_i and θ_i as defined earlier

$$h_{11} = \alpha_0 e^{j\theta_0} \qquad h_{12} = \alpha_1 e^{j\theta_1} \qquad h_{21} = \alpha_2 e^{j\theta_2} \qquad h_{22} = \alpha_3 e^{j\theta_3} \tag{10.5}$$

Here, $\boldsymbol{s_{wlan}}$ and $\boldsymbol{s_{bt}}$ are the discrete time signals derived from the continuous time as a result of matched filtering. The terms $\boldsymbol{w_1}, \boldsymbol{w_2}$ denote the AWGN noise components. Assuming channel information, the MRC estimate of $\boldsymbol{s_{wlan}}$ is calculated as,

$$\begin{aligned} \hat{\boldsymbol{s}}_{\mathbf{wlan}} &= {h_{11}}^* \boldsymbol{r_1} + {h_{12}}^* \boldsymbol{r_2} \\ &= (\underbrace{|h_{11}|^2}_{{\alpha_1}^2} + \underbrace{|h_{12}|^2}_{{\alpha_2}^2})\boldsymbol{s_{wlan}} + ({h_{11}}^* h_{21} + {h_{12}}^* h_{22})\boldsymbol{s_{bt}} + {h_{11}}^* \boldsymbol{w_1} + {h_{12}}^* \boldsymbol{w_2} \end{aligned} \tag{10.6}$$

Simplifying the above equation and adding the large scale fading coefficients as defined in Equation (10.2), we can obtain the MRC estimate of $\boldsymbol{s_{wlan}}$ as

$$\hat{\boldsymbol{s}}_{\mathbf{wlan}} = P_{wlan}\ ({\alpha_1}^2 + {\alpha_2}^2)\boldsymbol{s_{wlan}} + P_{bt}\ \tilde{\boldsymbol{s_{bt}}} + \tilde{\boldsymbol{w}} \tag{10.7}$$

where $\tilde{\boldsymbol{s_{bt}}} = ({h_{11}}^* h_{21} + {h_{12}}^* h_{22})\boldsymbol{s_{bt}}$ and $\tilde{\boldsymbol{w}} = {h_{11}}^* \boldsymbol{w_1} + {h_{12}}^* \boldsymbol{w_2}$.

The MRC makes the WLAN signal stronger giving a better performance over the single antenna receiver. In an 802.11b system the MRC can be considered a realistic case of a reverse transmission from say an 802.11b enabled Laptop/Desktop to the 802.11b router (AP) having 2 transmit antennas.

The improvement in the magnitude and the range of throughput for 1 Mbps BPSK scheme, resulting from MRC can be shown in Figure 10.4. The performance improvement is limited due to the presence of the Bluetooth interferer.

Similarly we present the results for the 11 Mbps CCK schemes as shown in Figure 10.5 below.

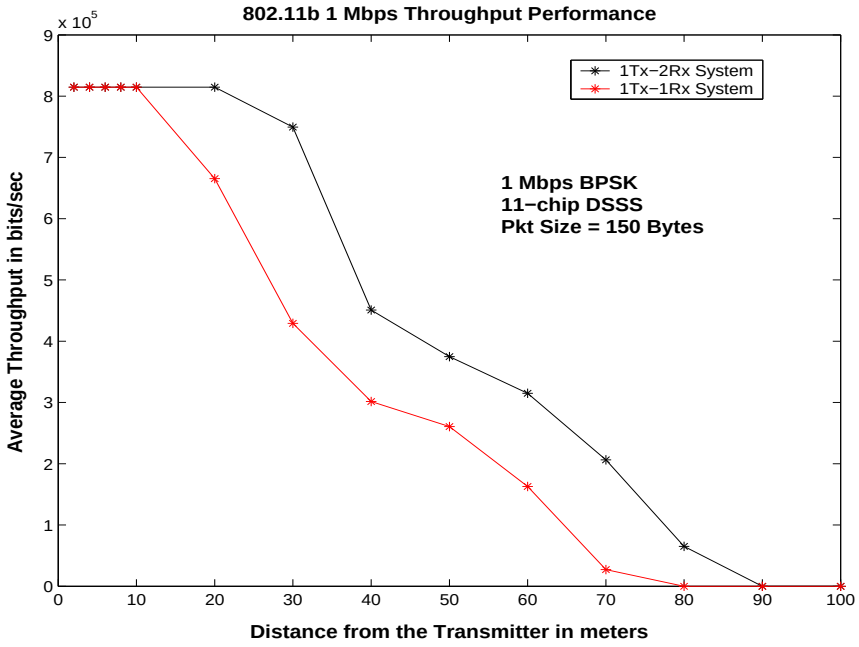

Figure 10.4: Throughput improvement of BPSK with Maximal Ratio Combining

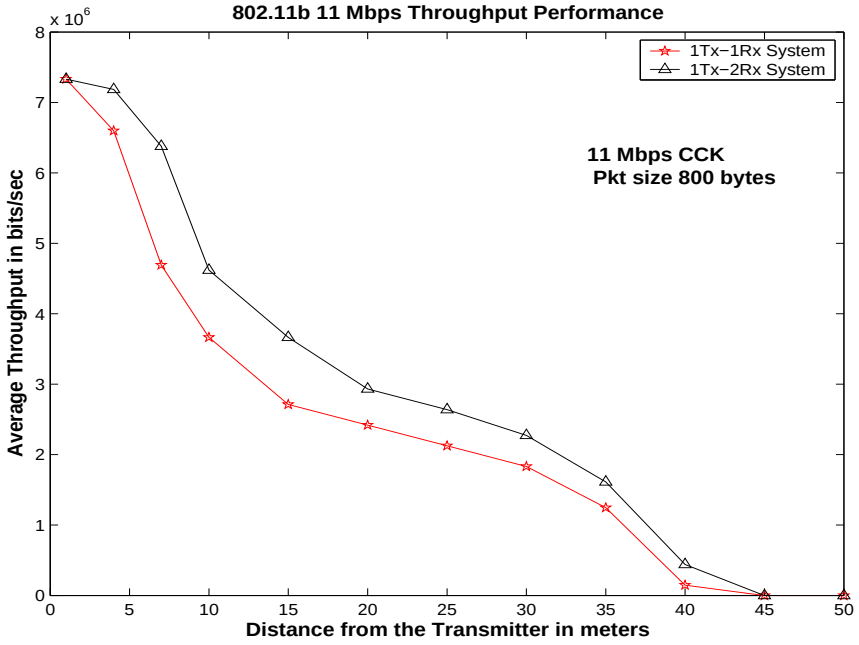

Figure 10.5: Throughput improvement of CCK with Maximal Ratio Combining

10.5 Throughput Improvement using Multiple Transmit Antennas - Space Time Coding Scheme

Some of the commercially available routers [6] deploy 2 transmit antennas as shown in Figure 10.6.

Figure 10.6: Commercially available 2 Transmit Antenna Routers [6]

The lower order modulation schemes used for these routers are BPSK and QQPSK as against the DPSK and DQPSK modulation schemes used for single antenna routers. The use of 2 transmit antennas motivates the use of Space Time Codes (STC)[7][38]. The 2 Transmit - 1 Receive antenna scheme shown in Figure 10.7 provides the same order diversity as that of an MRC with 1 Transmit and 2 Receive antennas. In this section we present the throughput of 1 Mbps BPSK using space time codes.

10.5.1 2 Branch Transmit - 1 Receive Scheme

Encoding and Transmission

In a given symbol period 2 signals are transmitted from 2 transmit antennas,namely s_0 from antenna 0 and s_1 from antenna 1 as shown in Table 10.1. In the next symbol period, the signals $-s_1^*$ and s_0^* are transmitted simultaneously from antennas 0 and 1. The space time codes are so called because of this type of encoding in space and time.

Table 10.1: Encoding and Transmission scheme

	antenna 0	antenna 1
time t	s_0	s_1
time t+T	$-s_1^*$	s_0^*

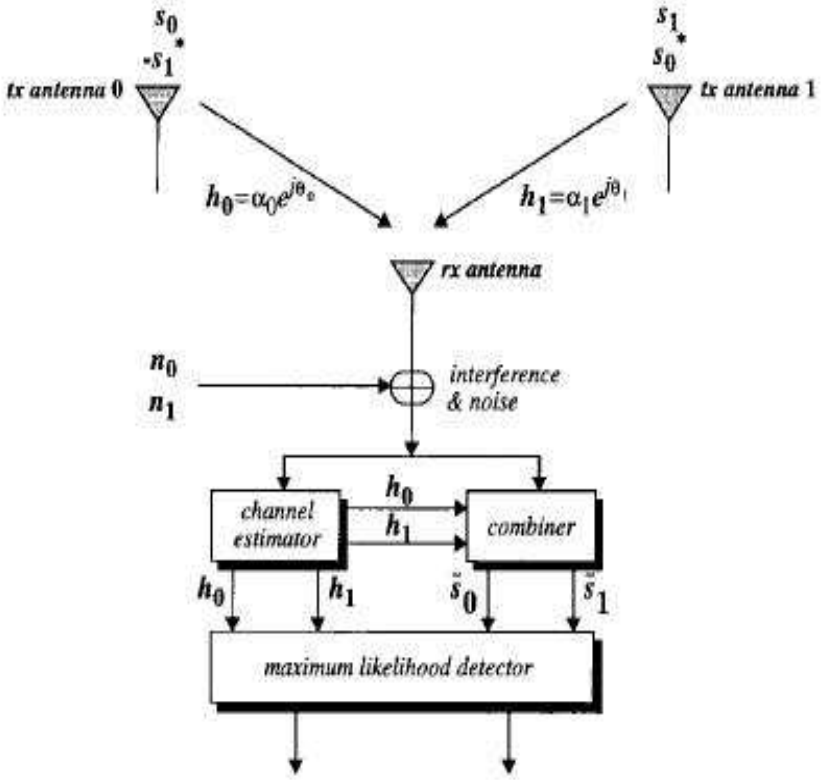

Figure 10.7: The 2 Transmit 1 Receive Antenna Scheme [7]

The channel coefficients h_0 and h_1 are assumed to be complex in nature. with the assumption that the channel is relatively slow and constant over 2 consecutive symbols we can write h_0 and h_1 as

$$h_0 = \alpha_0 e^{j\theta_0}$$

$$h_1 = \alpha_1 e^{j\theta_1} \tag{10.8}$$

where T is the symbol duration. The received signals can then be expressed as

$$\boldsymbol{r_0} = h_0 \boldsymbol{s_0} + h_1 \boldsymbol{s_1} + \boldsymbol{n_0}$$

$$\boldsymbol{r_1} = -h_0 \boldsymbol{s_1^*} + h_1 \boldsymbol{s_0^*} + \boldsymbol{n_1} \tag{10.9}$$

$\boldsymbol{r_0}$ and $\boldsymbol{r_1}$ are the received signals in time t and $t+T$ and $\boldsymbol{n_1}$ and $\boldsymbol{n_2}$ are the complex random noise variables comprising of the channel noise and BT interfering signal.

Signal Combining Scheme:

The signal combiner shown in Figure 10.7 constructs the signals $\tilde{s_0}$ and $\tilde{s_1}$ that are send to the maximum likelihood (ML) detector.

$$\boldsymbol{\tilde{s_0}} = h_0^* \boldsymbol{r_0} + h_1 \boldsymbol{r_1^*}$$

$$\boldsymbol{\tilde{s_1}} = h_1^* \boldsymbol{r_0} - h_0 \boldsymbol{r_1^*} \tag{10.10}$$

Hence from Equations (10.8), (10.9) and (10.10) we get

$$\boldsymbol{\tilde{s_0}} = ({\alpha_0}^2 + {\alpha_1}^2)\boldsymbol{s_0} + h_0^* \boldsymbol{n_0} + h_1 {\boldsymbol{n_1}}^*$$

$$\boldsymbol{\tilde{s_1}} = ({\alpha_0}^2 + {\alpha_1}^2)\boldsymbol{s_1} - h_0 {\boldsymbol{n_1}}^* + {h_1}^* \boldsymbol{n_0} \tag{10.11}$$

The ML detector then uses the appropriate decision rules to estimate s_0 and s_1. For the BPSK modulation used here, the decision rule is

$$\boldsymbol{\hat{s_0}} = \text{sign } \{\text{real}(\boldsymbol{\tilde{s_0}})\}$$

$$\boldsymbol{\hat{s_1}} = \text{sign } \{\text{real}(\boldsymbol{\tilde{s_1}})\} \tag{10.12}$$

The 2 transmit - 1 receive can be used in all the four modulation schemes namely BPSK, QPSK and CCK. Only the BPSK scheme has been simulated in this project. Figure 10.8 below shows the results for a 2 transmit 1 receive antenna scheme compared against the results obtained by the MRC 1 transmit and 2 receive and the 1 transmit 1 receive antennas schemes. As before, we simulate the presence of large scale fading given along with the small scale fading as given in Equation (10.2).

As before we select a packet size of 150 bytes and use DSSS spreading with the 11-chip Barker sequence as specified in the 802.11b standard. As seen from the graph the throughput performance by using 2 transmit 1 receive antennas is better than the one with 1 transmit and 1 receive antennas.

10.6 Error Detection and Correction

In this section, we discuss the effect of using error correction codes on the performance of the 802.11b Wireless LAN.

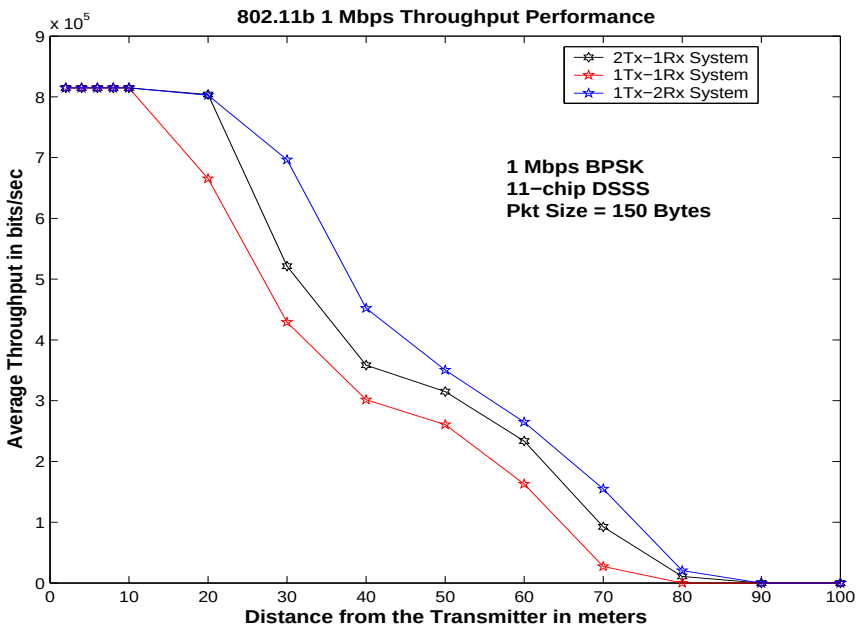

Figure 10.8: Performance of the 2 Transmit 1 Receive Antenna Scheme

The 802.11b system transmits data in packets. In the throughput simulations so far, an entire packet was discarded with the detection of even a single error in the packet. In the actual system implementation, an automatic repeat request (ARQ) will be used to retransmit any packets that contained errors detected by the cyclic redundancy check. However, throughput should increase if we are able to keep any packets in error by correcting the data in error instead of discarding the whole packet and re-transmitting everything. The use of error correction codes accounts for the error detection capability of the system and increases the number of correctable errors, giving a slight improvement in throughput.

10.6.1 Channel Coding Fundamentals

Channel coding introduces redundancies in the digital data in its attempt to reduce the number of errors in the data. The channel codes used to detect errors are called error detecting codes, while error correction codes are used to correct the errors.

According the Shannon, the number of errors induced by the channel can be effectively reduced to any desired extent by proper encoding of the data. The Shannon's channel

capacity formula applicable to AWGN channels [3] can be stated as

$$C = B\log_2\left(1 + \frac{P}{N_0 B}\right) = B\log_2\left(1 + \frac{S}{N}\right) \tag{10.13}$$

Here C is the channel capacity (in bits/sec), B is the transmission bandwidth (in Hz), P is the received signal power (in watts), and N_0 is the noise power spectral density (in Watts/Hz).

The power received at the receiver is given by

$$P = E_b R_b \tag{10.14}$$

Here E_b is the average bit energy and R_b is the bit rate. Thus we have,

$$\frac{C}{B} = \log_2\left(1 + \frac{E_b R_b}{N_0 B}\right) \tag{10.15}$$

C/B is the bandwidth efficiency. The introduction of data redundancies improves the performance of the wireless link. However, the introduction of redundancies increases the data rate, thus increasing the bandwidth requirement for a fixed source of data. This results in bandwidth efficiency reduction for higher SNRs, while giving an excellent performance at lower SNRs. The channel coder thus operates on a digital message to generate a code sequence of the data for transmission. The 3 basic types of error detection and correction codes are Block Codes, Convolutional Codes and Turbo Codes.

10.6.2 Error Correction in the 802.11b simulator

The implementation of error correction codes in the 802.11b simulator increases the complexity and is time consuming. Instead of coding the data, we assume the presence of error correction codes. Thus, instead of discarding a packet containing errors, we simulate the throughput for correctable error values of 10, 50 and 100 per packet and observe the improvement in performance. It should be noted here that, this is a generalized version of the effect of error correcting codes. More specific results can be obtained by using any of the above described error correction codes. The use of block codes and convolutional codes for throughput optimization would serve as an interesting problem for future analysis of the 802.11b Wireless LAN.

Figures 10.9 and 10.10 demonstrate the packet error rate and throughput optimization achieved for lower SNRs or higher distances as a result of error correction. As before we choose a packet size of 150 bytes with DSSS spreading and BPSK modulation.

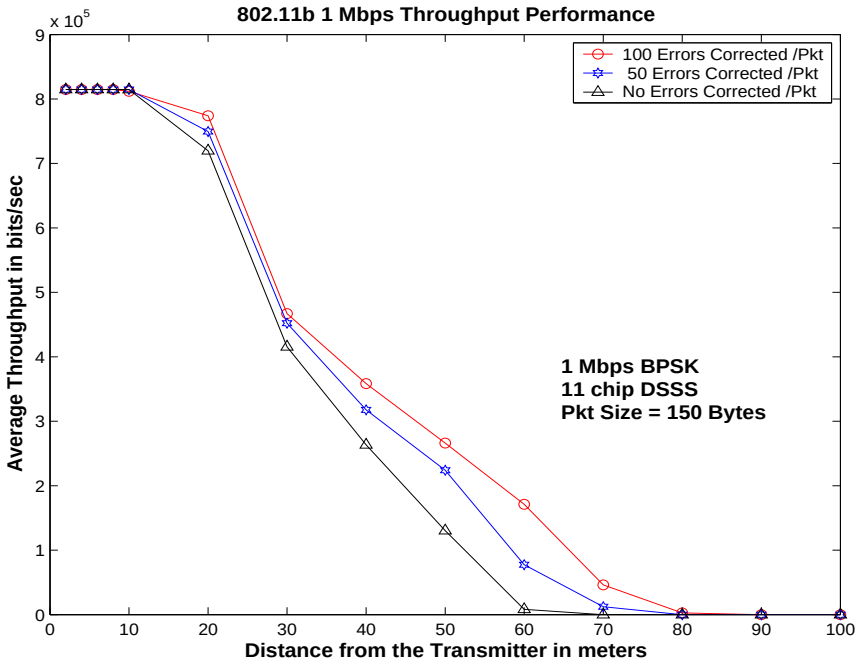

Figure 10.9: Throughput Optimization using error correction codes

10.7 Interference Suppression with Interference Cancellation (IC)

This section discusses and simulates the interference suppression technique as described by Henriksson [18]. For IC, we consider signal reception using 2 receiving antennas similar to MRC technique discussed before. In the previous simulations, we assumed that the receiver has perfect knowledge of the channel information. However in reality, this not being the case, we need to estimate the channel coefficients by training the system. The received training signal can be modelled in continuous time domain as

$$\boldsymbol{r}(t) = \boldsymbol{h}_T\, y(t) + \underbrace{\boldsymbol{h}_{bt}\, s_{bt}(t) + \boldsymbol{n}(t)}_{\boldsymbol{w}(t)} \tag{10.16}$$

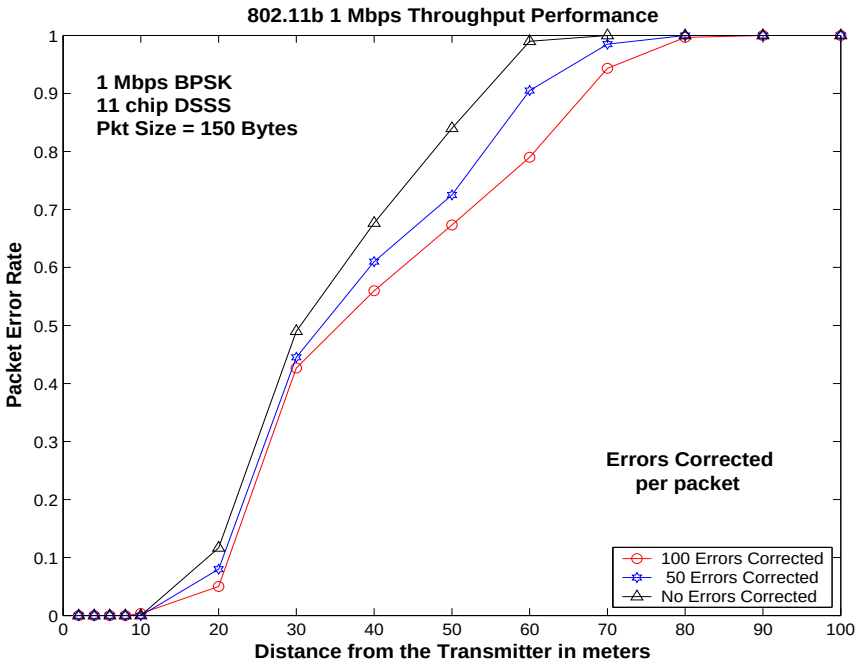

Figure 10.10: Packet Error Rates using error correction codes

where $\boldsymbol{r}(t) = [r_1(t)\ r_2(t)]^T$. $\boldsymbol{h}_T = [h_{11}\ \ h_{12}]^T$ represents the unknown channel vector for the WLAN training sequence $y(t)$, with $y(t)$ being the continuous time WLAN modulated signal similar to $s_{wlan}(t)$ described before. The channel vector for the Bluetooth signal is given by $\boldsymbol{h}_{bt}$, where $\boldsymbol{h}_{bt} = [h_{21}\ h_{22}]^T$. The AWGN noise $\boldsymbol{n}(t)$ is given as $\boldsymbol{n}(t) = [n_1(t)\ \ n_2(t)]^T$

The discrete time signal model for Equation (10.16) can be given as

$$\boldsymbol{R} = \boldsymbol{h}_T\,\boldsymbol{y}^T + \underbrace{\boldsymbol{h}_{bt}\,\boldsymbol{s_{bt}}^T + \boldsymbol{N}}_{\boldsymbol{W}}. \tag{10.17}$$

Here $[\boldsymbol{N}]_{ij} \sim \mathcal{N}_C(0, \frac{N_0}{2})$ and $\boldsymbol{R} \in \mathcal{C}^{2\times N}$ is defined by $[\boldsymbol{R}]_{1j} = \int_{(j-1)T}^{jT} r_1(t)\ \psi(t - jT)\,dt$, $[\boldsymbol{R}]_{2j} = \int_{(j-1)T}^{jT} r_2(t)\ \psi(t - jT)\,dt$, with pulse shape $\psi(t)$, packet length N. $\mathcal{C}$ denotes a matrix of complex elements.

Also, $\boldsymbol{y} = [y_1, y_2, ...y_N]^T$ is the discrete time vector of WLAN modulated symbols, and $\boldsymbol{s_{bt}} = [b_1, b_2, ...b_N]^T$ is the discrete time vector of GFSK modulated symbols. The channel vectors $\boldsymbol{h}_T$ and $\boldsymbol{h}_{bt}$ are as defined above with individual channel coefficients $h_{11}, h_{12}, h_{21}, h_{22}$ given by Equation (10.5).

Alternatively, the additive noise $\boldsymbol{W}$, representing both the background noise and the Bluetooth interference, can also be modelled as temporally white with some spatial color.

Thus we have $\boldsymbol{Q} = \boldsymbol{W}\boldsymbol{W}^H$ and $\boldsymbol{W} \in \mathcal{C}^{2\times N}$ where $\boldsymbol{W} = \boldsymbol{h}_{bt}\,\boldsymbol{s_{bt}}^T + \boldsymbol{N}$ with $\boldsymbol{Q}$ being the spatial noise covariance matrix.

The ML estimates [18] for $\boldsymbol{h}_T$ and $\boldsymbol{Q}$ can be found out as follows

$$\hat{\boldsymbol{h}}_T = \hat{\boldsymbol{r}}_{ry}\,\hat{r}_{yy}^{-1} \tag{10.18}$$

and

$$\hat{\boldsymbol{Q}} = \hat{\boldsymbol{R}}_{rr} - \hat{\boldsymbol{r}}_{ry}\,\hat{r}_{yy}^{-1}\,\hat{\boldsymbol{r}}_{ry}^{*} \tag{10.19}$$

where

$$\hat{\boldsymbol{R}}_{rr} = \frac{1}{N}\ \boldsymbol{R}\boldsymbol{R}^H$$

$$\hat{r}_{yy} = \frac{1}{N}\ \boldsymbol{y}^H\boldsymbol{y}$$

$$\hat{\boldsymbol{r}}_{ry} = \frac{1}{N}\ \boldsymbol{R}\boldsymbol{y}^{*} \tag{10.20}$$

The transmitted signal $\boldsymbol{s_{wlan}}$ can be estimated using $\hat{\boldsymbol{h}}_T$ and $\hat{\boldsymbol{Q}}$ as

$$\begin{aligned}\hat{\boldsymbol{s}}_{\boldsymbol{wlan}} &= \arg\min_{\boldsymbol{s_{wlan}}} \left|\left|\boldsymbol{R} - \hat{\boldsymbol{h}_T}\,\boldsymbol{s_{wlan}}^T\right|\right|^2_{\hat{\boldsymbol{Q}}} \\ &= \left(\boldsymbol{R} - \hat{\boldsymbol{h}_T}\,\boldsymbol{s_{wlan}}^T\right)^T \hat{\boldsymbol{Q}} \left(\boldsymbol{R} - \hat{\boldsymbol{h}_T}\,\boldsymbol{s_{wlan}}^T\right) \\ &= \left(\left(\hat{\boldsymbol{h}}_T^{*}\,\hat{\boldsymbol{Q}}^{-1}\,\hat{\boldsymbol{h}}_T\right)^{-1}\hat{\boldsymbol{h}}_T^{*}\,\hat{\boldsymbol{Q}}^{-1}\right)\boldsymbol{R}\end{aligned} \tag{10.21}$$

with $\hat{\boldsymbol{Q}}$ being the estimate of the noise covariance matrix $\boldsymbol{Q}$ defined earlier and $\hat{\boldsymbol{h}}_T$ being the estimate of the unknown channel matrix. The transmitted signal estimate $\hat{\boldsymbol{s}}_{\boldsymbol{wlan}}$ is the compared with the actual transmitted signal $\boldsymbol{s_{wlan}}$ to give an account of the performance of the interference suppression.

The improvement in throughput resulting from the IC scheme can be shown in Figure 10.11 below. As before, we simulate the large scale and the small scale fading models given in Equation (10.2). The IC scheme cancels out both the Bluetooth noise and the receiver noise, hence the performance is much better than the system without any interference cancellation and channel estimation. Here we consider 1 Mbps BPSK Modulation with packet size of 150 bytes. Similarly, we plot the results for 11 MBPS CCK modulation in Figure 10.12. The packet size used for 11 Mbps CCK was 800 bytes. As seen in both the cases, the degradation caused by the Bluetooth interferer is cancelled out to a great extent. This is because the channel is trained for a large amount of data; i.e. 150 bytes for BPSK and 800 bytes for CCK. This yields near exact estimates for the channel matrix $\hat{\boldsymbol{h}}_T$ and the spatial noise covariance

matrix $\hat{\boldsymbol{Q}}$. It would be worthwhile to note that, a certain amount of time is spent in training the data. However, in this simulation, we do not consider the effect of training time spent in reducing the actual data throughput.

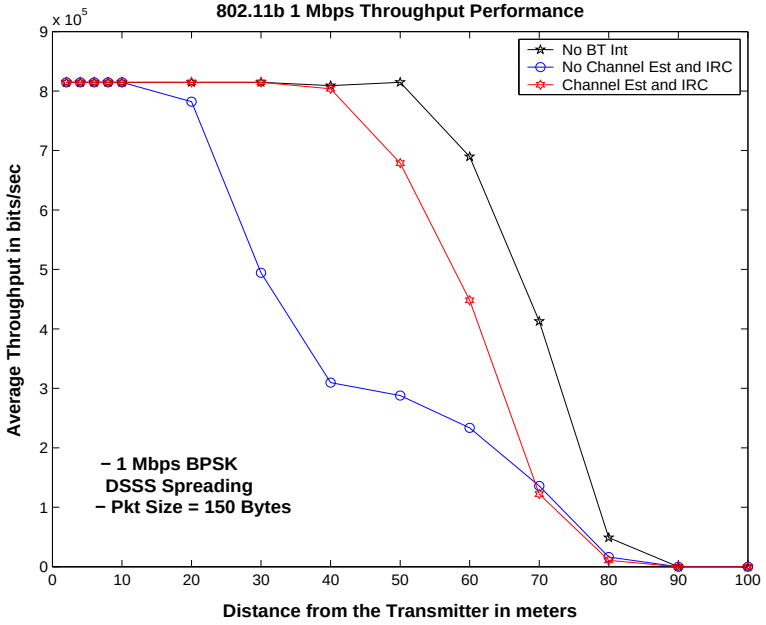

Figure 10.11: Interference Rejection in 802.11b: BPSK Modulation

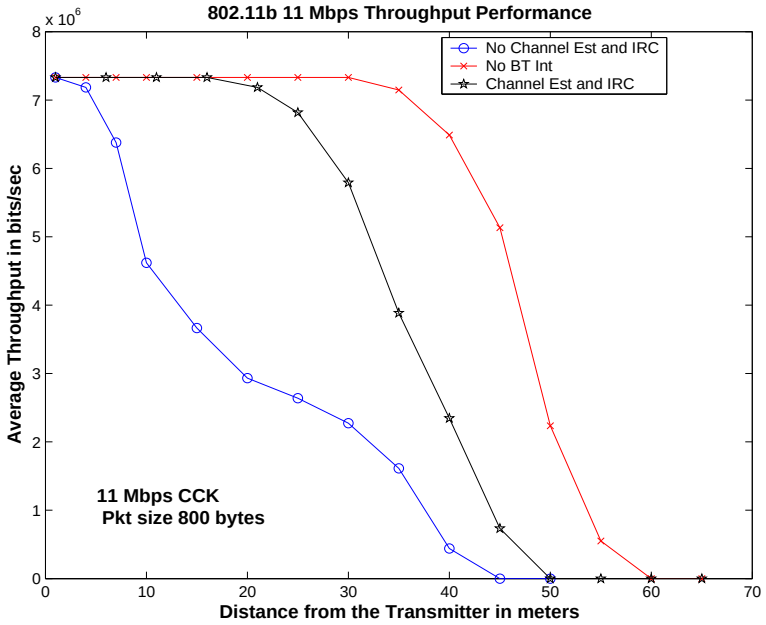

Figure 10.12: Interference Rejection in 802.11b: 11 Mbps CCK Modulation

10.8 Conclusions

This section explored the various receivers possible to maximize the performance of the IEEE 802.11b Wireless LAN. We observed the worst case, best case and the average throughput possible with the existence of a single bluetooth interferer. The scenario would change drastically due to the presence of multiple Bluetooth interferers. The improvement in throughput resulting from MRC and STC is observed. We present a general picture of the throughput optimization assuming the presence of error correction codes. Finally, we also attempted to cancel out the harmful effects of the BT interference and the receiver noise, by employing the interference cancellation technique. The concluding chapter discusses our final conclusions and future work possible in this area.

Chapter 11

Conclusions and Future Work

11.1 Conclusions and Future Work

In Chapter 10, we presented simulation results for throughput optimization using a variety of detection techniques. It should be noted that our work focusses on a single user system. The scenario would be different for a multiuser system. The channel model in our simulations is a slow flat fading channel. In reality, the change would exhibit different characteristics during different times of the day. Hence, we need to analyze the system supporting multiple users for different channel conditions. This fact motivates the future work possible in this area. The sections below discuss the Link Adaption Strategy, Use of Error Correction Coding and Actual Simulation of an Office Environment.

11.2 Link Adaption Strategy

As we already know, the IEEE 802.11b PHY transmits data at 4 different data rates. In the actual system, the PHY rate to be used for transmission at any instant is determined by the transmitting station. A typical wireless channel may vary over time due on account of factors like station mobility, time-varying interference, and location-dependent errors. It would be a good idea to choose the transmission rate in an adaptive manner for such time varying channels. The authors of the paper [39] present a link adaptation algorithm for improving the system throughput by adapting the transmission rate to the current link

condition. Since this algorithm is based on the received signal strength measured from the received frames, it does not require any change in the IEEE 802.11b WLAN Medium Access Control (MAC) protocol

It would be a good research project to implement the Link Adaption Algorithm, with different channel conditions.

11.3 Simulation of an Office Environment

Our work focussed on a single user environment, i.e., one user(STA) and one Access Point (AP). A typical office environment may exist in an Extended Service Set (ESS) configuration as described earlier. In such a configuration, we may have multiple APs and many STAs. Our work considers the effect of a single Bluetooth interferer. In an office environment, multiple Bluetooth interferers may exist. We can have BT enabled PDAs, mobile phones mainly concerned with Bluetooth data transmission, and Bluetooth radios with Bluetooth voice transmission. Each of these devices will have different network utilization and hence variable effects on the nearest WLAN network configuration. The possible presence of a microwave oven in the radius of the WLAN is also important, while considering the degradation of the WLAN. With a rare possibility, the existence of the newer generation cordless phones operating in the 2.4 GHz band are also likely to have some effect on the WLAN performance. Finally, the effects of an adjacent WLAN network should also be taken into consideration. It would be an interesting project to model the system using Simulink and analyze its performance before undertaking an actual simulation.

Therefore, we suggest implementing the typical office environment to get a clearer picture of the various interference issues in an WLAN network.

11.4 Error Correction Coding

The effect of error correction coding in optimizing the throughput for lower values of signal-to-noise ratio would be a challenging project in this area. Our work simples assumes the presence of error correction codes. It would be a good project to use specific error

correction codes like convolutional codes, block codes and implement decoding algorithms like the Viterbi Algorithm.

In addition, we also propose the implementation of the MAC layer standard, specifically the Collision Sense Multiple Access/ Collision Avoidance (CSMA/CA) protocol.

References

[1] M. Fainberg, "A Performance Analysis of the IEEE 802.11b Local Area Network in the Presence of Bluetoooth Personal Area Network," M.S. thesis, Polytechnic University, June 2001.

[2] L. Magnus, "Physical Layer Simulations of the IEEE 802.11b Wireless LAN standard," M.S. thesis, June 2001.

[3] T. S. Rappaport, *Wireless Communication Systems: Principles and Practice*, 2nd ed., Prentice Hall, 2001.

[4] J. Figueroa, B. Garon, B. Pearson and A. Petrick, "Brief tutorial on IEEE 802.11 wireless LANs," *Wireless Technologies China, Conference Proceedings*, pp. 1–7, Feburary 1999.

[5] P. Bhagwat, "Bluetooth: Technology for short-range wireless apps," *IEEE Internet Computing*, pp. pp. 96–103, June 2001.

[6] LinkSys Corp, http://www.tigerdirect.com, *Linksys Wireless B Broadband Router*.

[7] S. M. Alamouti, "A simple transmit diversity technique for wireless communications," in *IEEE Journal on Selected Areas in Communications*, October 1998, vol. 16, pp. 1451–1458.

[8] Bluetooth Special Interest Group, *Specifications of the Bluetooth System*, vol.1 v1.0b core and vol.2 v1.0b edition, December 1999.

[9] IEEE 802.11 Working Comittee, The Institute of Electrical and Electronics Engineers,USA , *IEEE Standard for Wireless LAN Medium Access Control (MAC) and Physical Layer (PHY) Specification*, 1 edition, June 1997.

[10] M. Takai, A. Lee and M. Gerla, "Impact of channel models on simulation of large scale wireless networks," in *ACM/IEEE MSWIM'99*, Seattle, WA, August 1999.

[11] N. Golmie, R.E. Van Dyck , and A. Soltanian, "Interference of Bluetooth and IEEE 802.11 : Simulation Modelling and Performamce Evaluation," *Proc. ACM Int. Workshop on Modeling, Analysis, and Simulation of Wireless and Mobile Systems, Rome, Italy* , July 2001.

[12] A. Kamerman, "Coexistance between Bluetooth and IEEE 802.11, CCK solutions to avoid mutual interference," *IEEE P802.11 Working Group Contribution, IEEE P802.11-00/162r0*, July 2000.

[13] G. Ennis, "Impact of Bluetooth on 802.11 Direct Sequence," *IEEE P802.11 Working Group Contribution*, vol. IEEE P802.11-98/319, September 1998.

[14] J. Zyren, "Reliability of IEEE 802.11 WLANs in the presence of Bluetooth Radios," *IEEE P802.11 Working Group Contribution, IEEE P802.15-99/073r0, Santa Rosa, California*, September 1999.

[15] S. Shellhammer, "Packet Error Rate of an IEEE 802.11 WLAN in the presence of Bluetooth," *IEEE P802.11 Working Group Contribution, IEEE P802.15-00/133r0, Seattle, Washington*, May 2000.

[16] C. F. Chiasserini and R. Rao, "Performance of IEEE 802.11 WLANs in a Bluetooth Environment," in *IEEE Wireless and Networking Conference, WCNC, Chicago,IL*, September 2000.

[17] N. Golmie and F. Mouveaux, "Interference in the 2.4 GHz ISM Band: Impact on Bluetooth access control performance," in *IEEE ICC'01, Helsinki, Finland*, June 2001.

[18] C. Henriksson, "Reducing Bluetooth interference with diversity techniques in IEEE 802.11b networks," M.S. thesis, Royal Institute of Technology, May 2002.

[19] I. Howitt, "Bluetooth Performance in the Presence of 802.11b WLAN," in *IEEE Trans Vehicular Technology*, November 2002, vol. 51, pp. 1640–1651.

[20] R. Jordan and C. Abdallah, "Wireless communications and networking: An overview," *IEEE Antennas and Propagation Magazine*, vol. vol.44, pp. pp.185–193, Feburary 2002.

[21] IEEE 802.11 Working Group, *IEEE, Wireless Media Access Control (MAC) and Physical Layer (PHY) Specification*, http://grouper.ieee.org/groups/802.15, p802.11d6.2 edition, July 1998.

[22] IEEE 802.15 Working Group, http://grouper.ieee.org/groups/802.15, *IEEE 802.15 Group Website*, Core Version 1.1 edition, Feburary 2001.

[23] W. C. Y. Lee, *Digital Communications*, New York, McGraw Hil, 4th edition, 2000.

[24] J.G. Proakis, *Digital Communications*, 3rd ed., New York, NY: McGraw-Hill, 1995.

[25] IEEE, Part 11, *Wireless LAN Medium Access Control (MAC) and Physical Layer (PHY) specifications: Higher-Speed Physical Layer Extension in the 2.4 GHz Band*, IEEE 802.11b Working Comittee, The Institute of Electrical and Electronics Engineers,USA, 11 edition, September 1999.

[26] C. Andren and M. Webster, "CCK Modulation delivers 11 Mbps for high rate IEEE 802.11 Extension," in *Wireless Symposium/Portable by Design Conference*, 1999, pp. 1–10.

[27] H. Martin, R. Franck, B. Gilles and D. Andrzej, "Performance Anomaly of 802.11b," Tech. Rep., LSR-LMAG Laboratory, Grenoble, France.

[28] 3com Corporation, "IEEE 802.11b Wireless LANs - Technical Paper," *3com Journal*, 2001.

[29] K. Sarinnapakorn, "IEEE 802.11b high rate wireless local area networks," March 15th 2001.

[30] S. M. Schwartz, "Frequency Hopping Spread Spectrum Vs Direct Sequence Spread Spectrum in the Broadband Wireless Access an WLAN areas," Sales report, Feburary 10th 2001.

[31] J. Sun, "Complementary Code Keying Modulation," Tech. Rep., West Virginia University, Wireless Comm Research Lab, 2002.

[32] W. S. Wang, "Bluetooth: A new era of connectivity," *IEEE Microwave*, vol. 3, pp. 38–42, September 2002.

[33] M. C. Valenti and M. Robert, "Improving the QoS of Bluetooth through turbo coding," *Proc. IEEE Military Commun. Conf. (MILCOM), (Anaheim, CA)*, October 2002.

[34] S. Hong and Y. Lee, "Fractionally-spaced differential detection of GFSK Signals with small h," *IECIE Trans. Commn.*, vol. E84-N, no. 12, December 2001.

[35] A. Soltanian and R.E. Van Dyck, "Performance of the Bluetooth system in fading dispersive channels and interference," *Proc. IEEE Globecom*, 2001.

[36] R. Saikat, L. D.H, Chang. S, N. Nguyen , *Gaussian Frequency Shift Keying (GFSK) modulation and demodulation.*

[37] "Collision course How Bluetooth interference impacts wireless LANs," Tech. Rep., Proxim Technologies, Sunnyvale, CA 94085, USA, 2001.

[38] V. Tarokh, H. Jafarkhani, and A. R. Calderbank, "Space time block codes from orthogonal designs," in *IEEE Trans. Inform. Theory*, July 1999, vol. 45, pp. 1456–1467.

[39] J. P. Pavon, S. Choi, "Link Adaptation Strategy for IEEE 802.11 WLAN via Received Signal Strength Measurement," in *IEEE International Conference on Communications.* Wireless Communication and Networking Philips Research USA, Multimedia and Wireless Networking Laboratory School of Electrical Engineering, May 2003, vol. 2, pp. 1108 – 1113.

[40] T. Moon and W. Stirling, *Mathematical Methods and Algorithms for Signal Processing*, 1st ed., Prentice-Hall, Upper Saddle River, NJ, USA., 2000.

[41] K. N. Modi, "Precoding for multi-antenna multi-user communications," M.S. thesis, Lane Department of Computer Science and Electrical Engineering, West Virginia University, May 2004.

[42] S. Verdú, *Multiuser Detection*, Cambridge, UK: Cambridge University Press, 1998.

A Discrete-Time Statistical Model for an Additive White Gaussian Noise (AWGN) Channel

A.1 Introduction

For any digital communication systems, the goal of the receiver is to detect the transmitted signal upon reception of the received signal embedded in the random channel noise. The transmitted bandpass signal $g(t)$, in any communication system is given by

$$g(t) = s_m(t) \exp\left(j2\pi f_c t\right), \qquad 0 \leq t \leq T_s, \tag{A-1}$$

where f_c is the carrier frequency, and $s_m(t)$ is the bandlimited information carrying signal more commonly referred as the baseband signal.

For digital communications the baseband signal $s_m(t)$ is chosen from a set of M signal waveforms $\{s_m(t), m = 1, 2, ..M, \}$ with each waveform being transmitted within the symbol interval of duration T. Specifically, we consider transmission of information over the interval $0 \leq t \leq T$.

The channel corrupts the signal by adding white noise as it arrives at the receiver. Hence, we can express the received signal as

$$r(t) = s_m(t) + n(t) \tag{A-2}$$

where $n(t)$ denotes a sample of the additive white gaussian noise (AWGN) process, with power spectral density $\frac{1}{2}N_0$ W/Hz.

We can conveniently divide the receiver into two parts - the signal demodulator and the detector. The demodulator converts the received signal $r(t)$ into an N dimensional vector $[r = r_1, r_2, ..., r_N]$, with N being the dimension of the transmitted signal waveforms. The detector makes a decision on the possibly transmitted signal from a set of M signal waveforms. In our problem report, we use the matched filter demodulation and detection to obtain an estimate of the transmitted signal.

A.2 The Matched Filter Demodulation and the Detection Process

The detection of continuous time signals is relatively complex. Thus instead of using $r(t)$ to detect $s_m(t)$, we aim to simplify the detection process by using a discrete-time model.

The transmitted signal can be represented as a discrete-time vector. We represent the transmitted signal $s_m(t)$ from the set $\{s_m(t), m = 1, 2, ..M, \}$. Each of the signals $s_m(t)$, can be represented as a discrete-time vector with respect to some basis of the set $\{s_1(t), s_2(t), ..., s_m(t)\}$.

The signals $p_1(t), \cdots, p_U(t)$ form an orthonormal basis of the set $\{s_1(t), s_2(t), ..., s_m(t)\}$ with U being the set dimensionality. The basis can be found using the Gram-Schmidt procedure [40] [41].

With the basis, we can now represent the transmitted signal as

$$s_m(t) = \sum_{u=1}^{U} s_m[u] p_u(t), \qquad m = 1, \cdots, M, \tag{A-3}$$

where

$$s_m[u] =< s_m(t), p_u(t) > . \tag{A-4}$$

with the symbol $< \cdot, \cdot >$ being the Euclidean inner product

Hence the transmitted signal $s_m(t)$ can be represented as discrete-time vector $\boldsymbol{s}_m$, i.e.,

$$s_m(t) \leftrightarrow \boldsymbol{s}_m, \tag{A-5}$$

with $\boldsymbol{s}_m = [s_m[1], \cdots, s_m[U]]^T$ being the vector corresponding to the decomposition of $s_m(t)$ with respect to the basis of the set $\{s_1(t), s_2(t), ..., s_m(t)\}$.

Using the basis signals $p_1(t), \cdots, p_U(t)$, the demodulator computes the vector of sufficient statistics to estimate the transmitted discrete time signal.

This vector of sufficient statistics is represented by $\boldsymbol{r}$, as follows

$$\begin{aligned} r[i] &= < r(t), p_i(t) > \\ &= s_m[i] + n[i], \end{aligned} \tag{A-6}$$

with $n[i] =< n(t), p_i(t) >$, the Additive White Gaussian noise sample. The vector $\boldsymbol{r}$ will be given as

$$\boldsymbol{r} = \boldsymbol{s_m} + \boldsymbol{n}, \tag{A-7}$$

where $\boldsymbol{n} = [n[1], \cdots, n[U]]^T$, is a Gaussian vector with identically distributed entries.

The vector $\boldsymbol{r}$, thus generated corresponds to the vector of sufficient statistics for $s_m(t)$ in the presence of background gaussian noise [24, 42] .

From(A-7), we can observe that discrete-time transmitted signal is $\boldsymbol{s}_m$ and the corresponding discrete-time received signal as formed by the demodulator is $\boldsymbol{r}$.

Thus the transmission and reception of continuous-time signals can be modelled as as discrete-time AWGN channel model with discrete-time input $\boldsymbol{s}_m$ and discrete-time output $\boldsymbol{r}$. This discrete time model is used through this problem report. For the detection process, the error minimizing detector will correspond to the ML detector. [24]

B The Discrete-Time Statistical Model for a Slow Fading Wireless Channel

B.1 Introduction

For discrete multipath channel the baseband received signal after down-conversion is represented as [24]

$$\begin{aligned} r(t) &= \left(\sum_i a_i(t) s_m(t - \tau_i(t)) \exp\left(j2\pi f_c(t - \tau_i(t))\right) + n'(t) \right) \exp(-j2\pi f_c t) + n_b(t) \\ &= \sum_i a_i(t) s_m(t - \tau_i(t)) \exp(-j2\pi f_c \tau_i(t)) + n(t), \end{aligned} \tag{B-8}$$

where $a_i(t)$ represents the time-varying path gain, $\tau_i(t)$ represents the time-varying path delay of the i^{th} path, f_c is the carrier frequency and $n(t)$ the noise at the output of the down-convertor.

Similarly, we can derive the continuous-time, bandlimited received signal as

$$r(t) = \int_{-\infty}^{\infty} a(\tau, t) s_m(t - \tau) \exp\left(-j2\pi f_c \tau\right) \mathrm{dt} + n(t). \tag{B-9}$$

with $a(\tau, t)$ being the time-varying path gain and τ representing the path delay.

Thus, we can model the wireless channel as a time-varying linear filter. In the remainder of the section we will derive the discrete-time statistical model for a flat fading wireless channel similar to the one obtained for an AWGN channel.

B.2 The Matched Filter Demodulation and the Detection Process

For wireless communication systems, we know that the channel, behaves similar to a complex Gaussian random process. The transmitted signal is thus filtered via a random process before arriving at the receiver as shown in (B-8) and (B-9), besides being embedded in noise.

For a signal in the continuous multipath channel as shown in (B-9), we can represent the signal $r(t)$ as the Fourier Transform of the transmitted signal $S_m(f)$, and the time-varying frequency response of the channel filter $H(f, t)$ [24]. Thus we have

$$r(t) = \int_{-\infty}^{\infty} H(f,t) S_m(f) \exp(j2\pi f t)\, \mathrm{df} + n(t). \tag{B-10}$$

Assuming that the channel is slow flat fading i.e. the channel is constant during the transmission of the signal $s_m(t)$, we can write the time-varying filter response as $H(f, t) = H(0, t) = h$. Thus we have

$$r(t) = h s_m(t) + n(t) \tag{B-11}$$

with, h being a complex Gaussian random variable, assuming the channel to be complex Gaussian.

As before, the output of the match filter k at the demodulator will be

$$\begin{aligned} r[k] &= < r(t), p_k(t) > \\ &= h s_m[k] + n[k]. \end{aligned} \tag{B-12}$$

Thus we can represent the discrete-time received signal at the output of the demodulator as

$$\boldsymbol{r} = h\boldsymbol{s_m} + \boldsymbol{n}. \tag{B-13}$$

The transmission and reception of continuous-time signals in a fading multipath channel can be modelled as as discrete-time slow fading channel model with discrete-time input $\boldsymbol{s}_m$ and discrete-time output $\boldsymbol{r}$. This discrete time model is used through this problem report. As before, for the detection process, the error minimizing detector will correspond to the ML detector. [24]